DESY 02-009
hep-ph/0201234
January 2002

ISSN 0418-9833

arXiv:hep-ph/0201234v2 21 May 2002

J/ψ Inclusive Production in νN Neutral-Current Deep-Inelastic Scattering

Bernd A. Kniehl and Lennart Zwirner
II. Institut für Theoretische Physik, Universität Hamburg,
Luruper Chaussee 149, 22761 Hamburg, Germany

Abstract

We calculate the cross section of J/ψ inclusive production in neutrino-nucleon deep-inelastic scattering via the weak neutral current within the factorization formalism of nonrelativistic quantum chromodynamics. Besides J/ψ single production via the Z-gluon fusion mechanism, we also consider J/ψ plus hadron-jet associated production. We take into account both direct production and feed-down from directly-produced heavier charmonia. We present theoretical predictions for the J/ψ transverse-momentum and rapidity distributions, which can be measured in the CHORUS and NOMAD experiments at CERN, including conservative error estimates. In order to interpret a recent CHORUS measurement of the total cross section, we also estimate the contribution due to J/ψ prompt production via diffractive processes using the vector-meson dominance model.

PACS numbers: 12.38.-t, 13.60.Hb, 13.60.Le, 14.40.Gx

1 Introduction

Since its discovery in 1974, the J/ψ meson has provided a useful laboratory for quantitative tests of quantum chromodynamics (QCD) and, in particular, of the interplay of perturbative and nonperturbative phenomena. The factorization formalism of nonrelativistic QCD (NRQCD) [1] provides a rigorous theoretical framework for the description of heavy-quarkonium production and decay. This formalism implies a separation of short-distance coefficients, which can be calculated perturbatively as expansions in the strong-coupling constant α_s, from long-distance matrix elements (MEs), which must be extracted from experiment. The relative importance of the latter can be estimated by means of velocity scaling rules, i.e. the MEs are predicted to scale with a definite power of the heavy-quark (Q) velocity v in the limit $v \ll 1$. In this way, the theoretical predictions are organized as double expansions in α_s and v. A crucial feature of this formalism is that it takes into account the complete structure of the $Q\overline{Q}$ Fock space, which is spanned by the states $n = {}^{2S+1}L_J^{(c)}$ with definite spin S, orbital angular momentum L, total angular momentum J, and colour multiplicity $c = 1, 8$. In particular, this formalism predicts the existence of colour-octet (CO) processes in nature. This means that $Q\overline{Q}$ pairs are produced at short distances in CO states and subsequently evolve into physical, colour-singlet (CS) quarkonia by the nonperturbative emission of soft gluons. In the limit $v \to 0$, the traditional CS model (CSM) [2] is recovered. The greatest triumph of this formalism was that it was able to correctly describe [3] the cross section of inclusive charmonium hadroproduction measured in $p\overline{p}$ collisions at the Fermilab Tevatron [4], which had turned out to be more than one order of magnitude in excess of the theoretical prediction based on the CSM.

In order to convincingly establish the phenomenological significance of the CO processes, it is indispensable to identify them in other kinds of high-energy experiments as well. Studies of charmonium production in ep photoproduction, ep and νN deep-inelastic scattering (DIS), e^+e^- annihilation, $\gamma\gamma$ collisions, and b-hadron decays may be found in the literature; see Ref. [5] and references cited therein. Here, N denotes a nucleon. Furthermore, the polarization of charmonium, which also provides a sensitive probe of CO processes, was investigated [6,7]. Until very recently, none of these studies was able to prove or disprove the NRQCD factorization hypothesis [1]. However, preliminary data of $\gamma\gamma \to J/\psi + X$ taken by the DELPHI Collaboration [8] at LEP2 provide first independent evidence for it [9].

In this paper, we revisit J/ψ inclusive production in νN DIS. In particular, we consider the process $\nu + N \to \nu + J/\psi + X$, which is mediated via the weak neutral current (NC). First experimental evidence for this process was delivered two decades ago by the CERN-Dortmund-Heidelberg-Saclay (CDHS) Collaboration, who exposed an iron target in the wide-band neutrino beam produced by protons from the CERN Super Proton Synchrotron (SPS) and identified the J/ψ mesons through their decays to $\mu^+\mu^-$ pairs [10]. Similar experiments are being performed by the NuTeV Collaboration at Femilab (Experiment E815) [11] and by the CHORUS [12] and NOMAD [13] Collaborations at CERN, using iron, lead, and iron targets, respectively. While NuTeV does not yet see evidence for NC production of J/ψ mesons, CHORUS nicely confirms the CDHS measurement. On the

other hand, NOMAD has not yet released any results on this.

The process $\nu+N \to \nu+J/\psi+X$ can either proceed diffractively or nondiffractively. In diffractive processes, the target nucleons interact with the rest of the process via exchanges of colourless objects with small spacelike virtualities t, and they typically stay intact (elastic scattering) or turn into a hadronic system of small invariant mass (diffractive dissociation). On the other hand, in nondiffractive processes, they participate in the hard scattering via their quark and gluon content and are thus destroyed (deep-inelastic scattering). In the case of elastic scattering off nucleons bound in compound nuclei, the recoiling nuclei can emerge unharmed (coherent scattering) or break up (quasielastic scattering).

The diffractive process $\nu + N \to \nu + J/\psi + N'$, where N' denotes a system with little or no excitation, was studied in the framework of the vector-meson dominance model (VDM) [14,15,16]. The nondiffractive process $\nu + N \to \nu + J/\psi + X$ was treated in the parton model of QCD endowed with two alternative approaches: on the basis of the so-called Z-gluon fusion mechanism [15,16,17] in the colour evaporation model based on local parton-hadron duality [18]; and in the CSM [19]. For reviews, see Refs. [16,20].

In all these processes, the J/ψ mesons can be produced either directly or via radiative or hadronic decays of heavier charmonia, such as χ_{cJ} and ψ' mesons, where $J = 0, 1, 2$. The respective decay branching fractions are $B(\chi_{c0} \to J/\psi + \gamma) = (0.66 \pm 0.18)\%$, $B(\chi_{c1} \to J/\psi + \gamma) = (27.3 \pm 1.6)\%$, $B(\chi_{c2} \to J/\psi + \gamma) = (13.5 \pm 1.1)\%$, and $B(\psi' \to J/\psi + X) = (55 \pm 5)\%$ [21]. It has become customary to collectively denote the J/ψ mesons produced directly or via the feed-down from heavier charmonia as prompt. If the νN centre-of-mass (CM) energy $\sqrt{S}$ is sufficiently large, $\sqrt{S} > 2M_B \approx 10.6$ GeV, then J/ψ mesons can also originate from weak decays of b hadrons produced through the process $\nu + N \to \nu + B + \bar{B} + X$ in diffractive or nondiffractive DIS. The corresponding decay branching fraction is $B(B \to J/\psi+X) = (1.16\pm0.10)\%$ [21]. In fixed-target experiments, the requisite incident-neutrino energy E is $E > (4M_B^2 - m^2)/(2m) \approx 59$ GeV, where m is the nucleon mass. In the case of the CERN wide-band neutrino beam, only an insignificant fraction, namely 7%, of the total flux satisfies this criterion [13]. Therefore and because of the smallness of $B(B \to J/\psi + X)$, J/ψ production through b-hadron decay should be greatly suppressed in the CHORUS and NOMAD experiments and is not considered here.

In this paper, we present complete and up-to-date predictions for prompt J/ψ production in νN NC DIS, including both the diffractive and nondiffractive contributions, which can be readily compared with available and expected CHORUS and NOMAD data. Specifically, we calculate the nondiffractive cross section of $\nu+N \to \nu+J/\psi+X$, where X denotes the nucleon remnant and possibly one additional hadron jet, to lowest order (LO) in the framework of the NRQCD factorization formalism [1], and we reanalyze the diffractive cross section of $\nu+N \to \nu+J/\psi+N'$ in the VDM adopting the results of Refs. [15,16] complemented with new input information. As for the nondiffractive direct contribution, our analysis is, in a way, complementary to the one of Ref. [22], where $e+p \to e+J/\psi+X$ via photons with large virtualities Q^2 was investigated: while the photon-quark coupling is purely vectorial, Z bosons couple to quarks mainly through axial-vector couplings,

the vector-coupling strengths being numerically small. However, by charge-conjugation invariance, the leading CSM prediction only involves vector couplings and may thus be obtained from Ref. [22] by appropriate substitutions [19]. As mentioned above, the non-diffractive prompt CS contribution was already studied in Ref. [19], two decades ago. However, since the authors of that paper did not present analytic results and used input parameters that are now obsolete, it is indispensable to repeat this analysis.

The leading MEs of the S-wave charmonia $\psi = J/\psi, \psi'$ are $\left\langle \mathcal{O}^{\psi}\left[{}^3S_1^{(1)}\right]\right\rangle$, $\left\langle \mathcal{O}^{\psi}\left[{}^1S_0^{(8)}\right]\right\rangle$, $\left\langle \mathcal{O}^{\psi}\left[{}^3S_1^{(8)}\right]\right\rangle$, and $\left\langle \mathcal{O}^{\psi}\left[{}^3P_J^{(8)}\right]\right\rangle$, with $J = 0, 1, 2$, while those of the P-wave charmonia χ_{cJ} are $\left\langle \mathcal{O}^{\chi_{cJ}}\left[{}^3P_J^{(1)}\right]\right\rangle$ and $\left\langle \mathcal{O}^{\chi_{cJ}}\left[{}^3S_1^{(8)}\right]\right\rangle$. They satisfy the multiplicity relations

$$\begin{aligned}
\left\langle \mathcal{O}^{\psi}\left[{}^3P_J^{(8)}\right]\right\rangle &= (2J+1)\left\langle \mathcal{O}^{\psi}\left[{}^3P_0^{(8)}\right]\right\rangle,\\
\left\langle \mathcal{O}^{\chi_{cJ}}\left[{}^3P_J^{(1)}\right]\right\rangle &= (2J+1)\left\langle \mathcal{O}^{\chi_{c0}}\left[{}^3P_0^{(1)}\right]\right\rangle,\\
\left\langle \mathcal{O}^{\chi_{cJ}}\left[{}^3S_1^{(8)}\right]\right\rangle &= (2J+1)\left\langle \mathcal{O}^{\chi_{c0}}\left[{}^3S_1^{(8)}\right]\right\rangle,
\end{aligned} \tag{1}$$

which follow to LO in v from heavy-quark spin symmetry.

At $\mathcal{O}(\alpha^2\alpha_s)$, where α is Sommerfeld's fine-structure constant, the Z-gluon fusion mechanism [15,16,17] is realized by the CO partonic subprocesses $\nu + g \to \nu + c\overline{c}[n]$, where $n = {}^1S_0^{(8)}, {}^3S_1^{(8)}, {}^3P_J^{(8)}$ [23]. In order to enable the production of the CS Fock states $n = {}^3S_1^{(1)}, {}^3P_J^{(1)}$, we need to allow for one additional gluon in the final state. The resulting LO CS partonic subprocesses, $\nu + g \to \nu + c\overline{c}[n] + g$, are of $\mathcal{O}(\alpha^2\alpha_s^2)$ (see Fig. 1) [19].

The cross sections of $\nu + g \to \nu + c\overline{c}\left[{}^3P_J^{(1)}\right] + g$ suffer from infrared (IR) singularities in the limit of the outgoing gluon being soft. This reflects a well-known conceptual deficiency of the CSM [2]. In the NRQCD framework [1], these IR singularities are factorized at some cut-off scale and absorbed into redefinitions of the CO MEs $\left\langle \mathcal{O}^{\chi_{cJ}}\left[{}^3S_1^{(8)}\right]\right\rangle$ that multiply the cross section of $\nu + g \to \nu + c\overline{c}\left[{}^3S_1^{(8)}\right]$. In turn, these CO MEs become scale dependent at $\mathcal{O}(\alpha_s)$ and satisfy appropriate evolution equations. The factorization is conveniently performed in dimensional regularization [24]. In Ref. [19], these IR singularities were not encountered because the hadronic recoil energy E_h was required to exceed some minimum value $E_h^{\min}$. However, a rapid rise of cross section with decreasing value of $E_h^{\min}$ was observed.

In the same order, we also have the CO partonic subprocesses $\nu + a \to \nu + c\overline{c}[n] + a$, where $a = q, \overline{q}, g$, with $q = u, d, s$, and $n = {}^1S_0^{(8)}, {}^3S_1^{(8)}, {}^3P_J^{(8)}$ (see Fig. 1). The cross sections of the latter are plagued by collinear singularities in the limit of vanishing $c\overline{c}$ transverse momentum $p_T^\star$ in the $Z^\star N$ CM frame. Here, $Z^\star$ denotes the virtual Z boson. These singularities could be avoided by introducing an appropriate cut on $p_T^\star$. In a full next-to-leading-order (NLO) analysis, they would be factorized at mass scale μ_f and absorbed into the bare parton density functions (PDFs) of the nucleon N so as to renormalize the latter.

In this paper, we provide analytical results for the cross sections of all the $2 \to 2$ and $2 \to 3$ partonic subprocesses enumerated above to LO within the NRQCD factorization

formalism [1]. In the $2 \to 2$ case, we found agreement with Eqs. (8) and (9) of Ref. [23][1], so that there is no need to list our formulas for the squared transition-matrix elements. We then calculate the inclusive cross section of prompt J/ψ production in nondiffractive νN NC DIS under CHORUS and NOMAD kinematic conditions to LO in NRQCD and the CSM. This involves the $2 \to 2$ CO processes of J/ψ, χ_{cJ}, and ψ' production and the $2 \to 3$ CS processes of J/ψ and ψ' production. As explained above, the $2 \to 3$ CS processes of χ_{cJ} production lie beyond the scope of the CSM. We also consider the distributions in the J/ψ transverse momentum p_T and rapidity y in the laboratory frame, which should be experimentally accessible.

Table 1: Relative importance, measured in powers of α_s and $v^2 \approx \alpha_s$, of the various nondiffractive J/ψ production channels according to the NRQCD counting rules. The entries are normalized to the direct $2 \to 3$ CS contribution, which is of $\mathcal{O}\left(\alpha^2 \alpha_s^2 v^3\right)$.

	J/ψ, ψ'	χ_{cJ}
$2 \to 2$ CO	$v^4/\alpha_s \approx \alpha_s$	$v^2/\alpha_s \approx 1$
$2 \to 3$ CS	1	$v^2 \approx \alpha_s$
$2 \to 3$ CO	$v^4 \approx \alpha_s^2$	$v^2 \approx \alpha_s$

The relative importance, measured in powers of α_s and $v^2 \approx \alpha_s$, of the various nondiffractive J/ψ production channels according to the NRQCD counting rules is represented in Table 1. The entries are normalized to the direct $2 \to 3$ CS contribution, which is of $\mathcal{O}\left(\alpha^2 \alpha_s^2 v^3\right)$. In addition, the feed-down channels are suppressed by the respective branching fractions. In fixed-target experiments, which are typically performed at low values of $\sqrt{S}$ [10,11,12,13], phase-space suppression comes in as another limiting factor. This affects the $2 \to 3$ processes more severely than the $2 \to 2$ ones. In fact, as will become apparent in Section 3, this is the reason why, in the case of direct J/ψ and ψ' production, the $2 \to 2$ CO contributions greatly exceed the $2 \to 3$ CS ones, although they are formally suppressed according to Table 1. If events of nondiffractive direct J/ψ and ψ' production could be identified experimentally, this would lend itself to a powerful discriminator between the CSM and NRQCD. Obviously, the $2 \to 3$ CO contributions, which are not included in our numerical analysis for the reasons explained above, would only provide minor corrections to their $2 \to 2$ counterparts, which make up the bulk of the NRQCD prediction.

This paper is organized as follows. In Section 2, we present, in analytic form, the cross sections of the partonic subprocesses enumerated above and explain how to calculate from them the total cross section of prompt J/ψ production in nondiffractive νN NC DIS as well as its p_T and y distributions. Lengthy expressions are relegated to the Appendix.

[1]There is a typographical error in the last equation of Eq. (9): $\left(Q^2 + 4m_c^2\right)^2$ in the denominator should be replaced by $\left(Q^2 + 4m_c^2\right)^4$.

For the reader's convenience, we also recall the cross-section formulas for prompt J/ψ production in diffractive νN NC DIS. In Section 3, we present our numerical results and compare them with recent CHORUS data. Our conclusions are summarized in Section 4.

2 Analytic results

In this section, we present our analytic results for the cross sections of $\nu+N \to \nu+H+j+X$ in nondiffractive DIS, which proceeds through the $2 \to 3$ partonic subprocesses $\nu + a \to \nu + c\bar{c}[n] + a$ mentioned in Section 1. Here, $H = J/\psi, \chi_{cJ}, \psi'$, the hadron jet j arises from the fragmentation of the additional final-state parton a, and X is the nucleon remnant. In our numerical analysis, we only consider the CS processes of J/ψ and ψ' production and integrate their cross sections over all kinematically allowed values of the j three-momentum. The CS processes of χ_{cJ} production and the CO processes are provided for future applications. At the end of this section, we also present formulas for the cross sections of the processes $\nu + N \to \nu + H + X$ and $\nu + N \to \nu + H + N'$.

We work at LO in the parton model of QCD with $n_f = 3$ active quark flavours and employ the NRQCD factorization formalism [1] to describe the formation of the H meson. We start by defining the kinematics. As indicated in Fig. 2, we denote the four-momenta of the incoming neutrino and nucleon and the outgoing neutrino, H meson, and hadron jet by k, P, k', p_H, and p', respectively. The parton struck by the virtual Z boson carries four-momentum $p = xP$. We neglect the masses of the nucleon and the light quarks, call the one of the H meson M, and take the charm-quark mass to be $m_c = M/2$. In our approximation, the nucleon remnant X has zero invariant mass, $M_X^2 = (P - p)^2 = 0$. The CM energy square of the νN collision is $S = (k + P)^2$. The virtual Z boson has four-momentum $q = k - k'$. As usual, we define $Q^2 = -q^2 > 0$, $y = q \cdot P/k \cdot P$, and the inelasticity variable $z = p_H \cdot P/q \cdot P$. In the nucleon rest frame, y and z measure the relative neutrino energy loss and the fraction of the $Z^\star$ energy transferred to the H meson, respectively. The $Z^\star N$ CM energy square is $W^2 = (q + P)^2 = yS - Q^2$. The system X' consisting of j and X has invariant mass square $M_{X'}^2 = (q+P-p_H)^2 = (1-x)y(1-z)S$. As usual, we define the partonic Mandelstam variables as $\hat{s} = (q + p)^2 = xyS - Q^2$, $\hat{t} = (q - p_H)^2 = -xy(1 - z)S$, and $\hat{u} = (p - p_H)^2 = M^2 - xyzS$. By four-momentum conservation, we have $\hat{s} + \hat{t} + \hat{u} = M^2 - Q^2$. In the $Z^\star N$ CM frame, the H meson has transverse momentum and rapidity

$$p_T^\star = \frac{\sqrt{\hat{t}\,(\hat{s}\hat{u} + Q^2M^2)}}{\hat{s} + Q^2}, \tag{2}$$

$$y_H^\star = \frac{1}{2} \ln \frac{\hat{s}\,(M^2 - \hat{u})}{\hat{s}\left(M^2 - \hat{t}\right) + Q^2M^2} + \frac{1}{2} \ln \frac{W^2}{\hat{s}}, \tag{3}$$

respectively. Here and in the following, we denote the quantities referring to the $Z^\star N$ CM frame by an asterisk. The second term on the right-hand side of Eq. (3) originates from the Lorentz boost from the $Z^\star a$ CM frame to the $Z^\star N$ one. Here, $y_H^\star$ is taken to be positive in the direction of the three-momentum of the virtual Z boson.

In the parton model, the nucleon is characterized by its PDFs $f_{a/N}(x,\mu_f)$, and, at LO, an outgoing parton may be identified with a hadron jet. Thus, we have

$$d\sigma(\nu + N \to \nu + H + j + X) = \int_0^1 dx \sum_a f_{a/N}(x,\mu_f) d\sigma(\nu + a \to \nu + H + a), \quad (4)$$

where $a = u, \overline{u}, d, \overline{d}, s, \overline{s}, g$. Furthermore, according to the NRQCD factorization formalism [1], we have

$$d\sigma(\nu + a \to \nu + H + a) = \sum_n \left\langle \mathcal{O}^H[n] \right\rangle d\sigma(\nu + a \to \nu + c\overline{c}[n] + a), \quad (5)$$

where, to LO in v, $n = {}^3S_1^{(1)}, {}^1S_0^{(8)}, {}^3S_1^{(8)}, {}^3P_J^{(8)}$ for $H = J/\psi, \psi'$ and $n = {}^3P_J^{(1)}, {}^3S_1^{(8)}$ for $H = \chi_{cJ}$.

Decomposing the transition-matrix element of the partonic subprocess $\nu + a \to \nu + c\overline{c}[n] + a$ into a leptonic part,

$$\mathcal{T}^\mu(\nu \to \nu + Z^\star) = -i \frac{g}{q^2 - M_Z^2} \overline{u}(k') \gamma^\mu \frac{1 - \gamma_5}{2} u(k), \quad (6)$$

where $g = 2^{1/4} G_F^{1/2} M_Z$, with G_F being Fermi's constant, and a hadronic one, $\mathcal{T}^\mu(Z^\star + a \to c\overline{c}[n] + a)$, from which the virtual Z-boson leg is amputated, we can write its cross section as

$$d\sigma(\nu + a \to \nu + c\overline{c}[n] + a) = \frac{1}{2xS} \frac{1}{2N_a} \frac{g^2}{\left(q^2 - M_Z^2\right)^2} \operatorname{tr}\left(\not{k} \gamma^\nu \frac{1 - \gamma_5}{2} \not{k}' \gamma^\mu \frac{1 - \gamma_5}{2} \right) H_{\mu\nu} \times d\mathrm{PS}_3(k + p; k', p_H, p'), \quad (7)$$

where $N_q = N_{\overline{q}} = N_c = 3$ and $N_g = (N_c^2 - 1)$ are the colour multiplicities of the partons a and the hadronic tensor $H^{\mu\nu}$ is obtained by summing the absolute square of $\mathcal{T}^\mu(Z^\star + a \to c\overline{c}[n] + a)$ over the spin and colour states of the incoming and outgoing partons a. Here and in the following, we employ the Lorentz-invariant phase-space measure

$$d\mathrm{PS}_n(p; p_1, \ldots, p_n) = (2\pi)^4 \delta^{(4)}\left(p - \sum_{i=1}^n p_i \right) \prod_{i=1}^n \frac{d^3 p_i}{(2\pi)^3 2 p_i^0}. \quad (8)$$

The first factor on the right-hand side of Eq. (7) stems from the flux and the second one from the average over the spin and colour states of the incoming parton. Integrating over the azimuthal angle of the outgoing neutrino, we may simplify Eq. (7) to become

$$d\sigma(\nu + a \to \nu + c\overline{c}[n] + a) = \frac{1}{2xS} \frac{1}{2N_a} \left(\frac{g}{4\pi} \right)^2 L^{\mu\nu} H_{\mu\nu} \frac{dy}{y} \frac{Q^2 dQ^2}{\left(Q^2 + M_Z^2\right)^2} d\mathrm{PS}_2(q + p; p_H, p'), \quad (9)$$

where

$$L^{\mu\nu} = \frac{1 + (1 - y)^2}{y} \epsilon_T^{\mu\nu} - \frac{4(1 - y)}{y} \epsilon_L^{\mu\nu} + (2 - y) \epsilon_A^{\mu\nu}, \quad (10)$$

with

$$\epsilon_T^{\mu\nu} = -g^{\mu\nu} + \frac{1}{q\cdot p}(q^\mu p^\nu + p^\mu q^\nu) - \frac{q^2}{(q\cdot p)^2}p^\mu p^\nu,$$
$$\epsilon_L^{\mu\nu} = \frac{1}{q^2}\left(q - \frac{q^2}{q\cdot p}p\right)^\mu \left(q - \frac{q^2}{q\cdot p}p\right)^\nu,$$
$$\epsilon_A^{\mu\nu} = \frac{i}{q\cdot p}\epsilon^{\mu\nu\rho\sigma}q_\rho p_\sigma \tag{11}$$

is the leptonic tensor. Here, we adopt the convention $\epsilon_{0123} = 1$. The cross section of $\overline{\nu} + a \to \overline{\nu} + c\overline{c}[n] + a$ emerges from Eq. (9) through crossing symmetry, by flipping the sign of the last term on the right-hand side of Eq. (10). In the following, the symbol ν collectively denotes neutrinos and antineutrinos.

We evaluate the cross sections of the relevant partonic subprocesses $\nu + a \to \nu + c\overline{c}[n] + a$ from Eq. (9) applying the covariant-projector method of Ref. [25]. Our results can be written in the form

$$\frac{d^3\sigma}{dy\,dQ^2\,d\hat{t}}(\nu + a \to \nu + c\overline{c}[n] + a) = F_a[n]\left[\frac{1+(1-y)^2}{y}T_a[n] - \frac{4(1-y)}{y}L_a[n] + (2-y)A_a[n]\right], \tag{12}$$

where $F_a[n]$, $T_a[n]$, $L_a[n]$, and $A_a[n]$ are functions of $\hat{s}$, $\hat{t}$, $\hat{u}$, and Q^2, which are listed in the Appendix. We combined the results proportional to the CO MEs $\left\langle \mathcal{O}^\psi\left[{}^3P_J^{(8)}\right]\right\rangle$ and $\left\langle \mathcal{O}^{\chi_{cJ}}\left[{}^3S_1^{(8)}\right]\right\rangle$ exploiting the multiplicity relations of Eq. (1). The $T_a[n]$ and $L_a[n]$ functions involve terms proportional to $v_i v_j$ or $a_i a_j$, while the $A_a[n]$ functions involve terms proportional to $v_i a_j$, where $i, j = q, c$. Here, $v_q = I_q^3 - 2e_q \sin^2\theta_w$ and $a_q = I_q^3$ are the $Zq\overline{q}$ vector and axial-vector couplings, respectively, where I_q^3 is the third component of weak isospin of the left-handed component of quark q, e_q is the fractional electric charge of the latter, and θ_w is the weak mixing angle. We recover our result for the cross section of $e + a \to e + J/\psi + a$, given in Eq. (13) of Ref. [22], by substituting in Eq. (12) $g = e$, $v_q = e_q$, $v_c = e_c$, $a_q = a_c = 0$, and $M_Z = 0$, where $e = \sqrt{4\pi\alpha}$ is the electron-charge magnitude.

For the CO Fock states $n = {}^1S_0^{(8)}, {}^3S_1^{(8)}, {}^3P_J^{(8)}$, the cross sections of Eq. (12) exhibit collinear singularities in the limit $\hat{t} \to 0$. According to the factorization theorem, the limiting expressions must coincide with the respective $\nu + g \to \nu + c\overline{c}[n]$ cross sections [23] multiplied by the spacelike $a \to g$ splitting functions. This provides another nontrivial check for our results.

It is interesting to observe that the cross sections of $\nu + g \to \nu + c\overline{c}\left[{}^3P_J^{(1)}\right] + g$ vanish in the limit $y \to 0$ and $Q^2 \to 0$.

Inserting Eq. (5) in Eq. (4) and including the maximum boundaries of the integrations over x and $\hat{t}$, we obtain

$$\frac{d^2\sigma}{dy\,dQ^2}(\nu + N \to \nu + H + j + X) = \int_{(Q^2+M^2)/(yS)}^1 dx \int_{-(\hat{s}+Q^2)(\hat{s}-M^2)/\hat{s}}^0 d\hat{t}$$

$$\times \sum_a f_{a/N}(x,\mu_f) \sum_n \left\langle \mathcal{O}^H[n] \right\rangle \frac{d^3\sigma}{dy\, dQ^2\, d\hat{t}}(\nu + a \to \nu + c\overline{c}[n] + a), \tag{13}$$

where $\left(d^3\sigma/dy\, dQ^2\, d\hat{t}\right)(\nu + a \to \nu + c\overline{c}[n] + a)$ is given by Eq. (12). The kinematically allowed ranges of S, y, and Q^2 are $S > M^2$, $M^2/S < y < 1$, and $0 < Q^2 < yS - M^2$, respectively. We then evaluate the cross section of prompt J/ψ production as

$$\begin{aligned} d\sigma(\nu + N \to \nu + (J/\psi)_{\text{prompt}} + j + X) &= d\sigma(\nu + N \to \nu + J/\psi + j + X) \\ &+ \sum_{J=0}^{2} B(\chi_{cJ} \to J/\psi + \gamma) d\sigma(\nu + N \to \nu + \chi_{cJ} + j + X) \\ &+ B(\psi' \to J/\psi + X) d\sigma(\nu + N \to \nu + \psi' + j + X). \end{aligned} \tag{14}$$

The distributions in y and Q^2 can be evaluated from Eq. (13) as it stands. It is also straightforward to obtain the distributions in $p_T^\star$ and $y_H^\star$, given in Eqs. (2) and (3), respectively, by accordingly redefining and reordering the integration variables in Eq. (13). The distribution in the J/ψ azimuthal angle $\phi^\star$ in the $Z^\star N$ CM frame is constant.

The evaluation of the distributions in the J/ψ transverse momentum p_T, rapidity y_H, and azimuthal angle ϕ in the laboratory frame is somewhat more involved. Choosing a suitable coordinate system in the $Z^\star N$ CM frame, we have

$$\begin{aligned} (k^\star)^\mu &= \frac{S - Q^2}{2W} \begin{pmatrix} 1 \\ \sin\psi^\star \\ 0 \\ \cos\psi^\star \end{pmatrix}, \qquad (k'^\star)^\mu = \frac{S - W^2}{2W} \begin{pmatrix} 1 \\ \sin\theta^\star \\ 0 \\ \cos\theta^\star \end{pmatrix}, \\ (q^\star)^\mu &= \frac{1}{2W} \begin{pmatrix} W^2 - Q^2 \\ 0 \\ 0 \\ W^2 + Q^2 \end{pmatrix}, \qquad (P^\star)^\mu = \frac{W^2 + Q^2}{2W} \begin{pmatrix} 1 \\ 0 \\ 0 \\ -1 \end{pmatrix}, \\ (p_H^\star)^\mu &= \begin{pmatrix} m_T^\star \cosh y_H^\star \\ p_T^\star \cos\phi^\star \\ p_T^\star \sin\phi^\star \\ m_T^\star \sinh y_H^\star \end{pmatrix}, \end{aligned} \tag{15}$$

where[2]

$$\begin{aligned} \cos\psi^\star &= \frac{2SW^2}{(S - Q^2)(W^2 + Q^2)} - 1, \qquad \cos\theta^\star = 1 - \frac{2SQ^2}{(S - W^2)(W^2 + Q^2)}, \\ m_T^\star &= \sqrt{M^2 + (p_T^\star)^2}. \end{aligned} \tag{16}$$

On the other hand, in the laboratory frame, which coincides with the nucleon rest frame,

[2]The formula for $\cos\theta^\star$ given in Ref. [22] contains a sign error, which was absent in the preprint version of that paper.

we have

$$k^\mu = E \begin{pmatrix} 1 \\ 0 \\ 0 \\ 1 \end{pmatrix}, \qquad (k')^\mu = E' \begin{pmatrix} 1 \\ \sin\theta \\ 0 \\ \cos\theta \end{pmatrix},$$
$$q^\mu = \begin{pmatrix} q^0 \\ -q\sin\psi \\ 0 \\ q\cos\psi \end{pmatrix}, \qquad P^\mu = m \begin{pmatrix} 1 \\ 0 \\ 0 \\ 0 \end{pmatrix},$$
$$p_H^\mu = \begin{pmatrix} m_T \cosh y_H \\ p_T \cos\phi \\ p_T \sin\phi \\ m_T \sinh y_H \end{pmatrix}, \tag{17}$$

where

$$E = \frac{S - m^2}{2m}, \qquad E' = \frac{S - W^2 - Q^2}{2m}, \qquad \cos\theta = 1 - \frac{2Q^2 m^2}{(S-m^2)(S-W^2-Q^2)},$$
$$q^0 = \frac{W^2 + Q^2 - m^2}{2m}, \qquad q = \sqrt{Q^2 + (q^0)^2},$$
$$\cos\psi = \frac{1}{q}\left(\frac{W^2+Q^2-m^2}{2m} + \frac{Q^2 m}{S-m^2}\right), \qquad m_T = \sqrt{M^2 + p_T^2}. \tag{18}$$

Notice that y_H is taken to be positive in the direction of the three-momentum of the incoming neutrino. Without loss of generality, we may require that $0 \le \psi^\star, \psi \le \pi$, for, otherwise, we can achieve this by rotating the respective coordinate systems by 180° around the z axis. We can then evaluate p_T, y_H, and ϕ from $p_T^\star$, $y_H^\star$, and $\phi^\star$ as

$$p_T = \sqrt{\left(p_T^\star\right)^2 + A\,(A - 2p_T^\star \cos\phi^\star)}, \tag{19}$$
$$y_H = y_H^\star + \ln\frac{(W^2+Q^2)m_T^\star}{\sqrt{S}W m_T} + \frac{1}{2}\ln\frac{S}{m^2}, \tag{20}$$
$$\cos\phi = \frac{p_T^\star \cos\phi^\star - A}{p_T}, \tag{21}$$

where

$$A = \frac{m_T^\star \exp(y_H^\star)\sin\psi^\star}{1+\cos\psi^\star} = \sqrt{\frac{Q^2(S-W^2-Q^2)}{SW^2}}\, m_T^\star \exp(y_H^\star). \tag{22}$$

The third term on the right-hand side of Eq. (20) stems from the Lorentz boost from the νN CM frame to the laboratory one. Since p_T, y_H, and ϕ depend on $\phi^\star$, the integration over $\phi^\star$ in Eq. (13) is no longer trivial, and we need to insert the symbolic factor $(1/2\pi)\int_0^{2\pi} d\phi^\star$ on the right-hand side of that equation.

For future applications, we also present compact formulas that allow us to determine $p_T^\star$, $y_H^\star$, and $\phi^\star$, once p_T, y_H, and ϕ are given. In fact, Eqs. (19) and (21) can be straightforwardly inverted by observing that the quantity A defined in Eq. (22) can be expressed in terms of m_T and y_H by substituting Eq. (20), the result being

$$A = \frac{m m_T \exp(y_H)}{W^2 + Q^2} \sqrt{\frac{Q^2}{S}(S - W^2 - Q^2)}. \tag{23}$$

Having obtained $p_T^\star$, we can then evaluate $y_H^\star$ from Eq. (20). For the reader's convenience, we collect the relevant formulas here:

$$\begin{aligned} p_T^\star &= \sqrt{p_T^2 + A(A + 2p_T \cos\phi)}, \\ y_H^\star &= y_H + \ln \frac{\sqrt{S} W m_T}{(W^2 + Q^2) m_T^\star} + \frac{1}{2} \ln \frac{m^2}{S}, \\ \cos\phi^\star &= \frac{p_T \cos\phi + A}{p_T^\star}. \end{aligned} \tag{24}$$

If the four-momentum $p_H + p' + P - p$ of the hadronic final state $H + j + X$ can be measured in the laboratory frame, then the $Z^\star$ four-momentum can be evaluated as $q = (p_H + p' + P - p) - P$. Since the direction of the incident neutrino beam is given by the experimental set-up, the four-momenta k and k' of the incident and scattered neutrinos can thus be reconstructed using Eqs. (17) and (18). Then, the $Z^\star N$ CM frame is well-defined, and $p_T^\star$, $y_H^\star$, and $\phi^\star$ can be determined. However, if the hadronic final state cannot be fully detected, then one can still measure p_T, y_H, and ϕ in the laboratory frame.

We now turn to the cross section of $\nu + N \to \nu + H + X$ in nondiffractive DIS, which proceeds through the $2 \to 2$ partonic subprocesses $\nu + g \to \nu + c\bar{c}[n]$ mentioned in Section 1. We have

$$\begin{aligned} \frac{d\sigma}{dQ^2}(\nu + N \to \nu + H + X) = {} & \frac{g^4 \alpha_s}{6M^3 \left(Q^2 + M_Z^2\right)^2} \int_{(Q^2+M^2)/S}^1 dx\, f_{g/N}(x, \mu_f) \\ & \times \sum_n \left\langle \mathcal{O}^H[n] \right\rangle h_n(y, Q^2), \end{aligned} \tag{25}$$

where, to LO in v, $n = {}^1S_0^{(8)}, {}^3S_1^{(8)}, {}^3P_J^{(8)}$ for $H = J/\psi, \psi'$ and $n = {}^3S_1^{(8)}$ for $H = \chi_{cJ}$. The functions $h_n(y, Q^2)$ may be found in Eq. (9) of Ref. [23], which contains a typographical error, as pointed out in Section 1. The kinematically allowed ranges of S and Q^2 are $S > M^2$ and $0 < Q^2 < S - M^2$, respectively. The kinematics of $\nu + N \to \nu + H + X$ emerges from that of $\nu + N \to \nu + H + j + X$ by nullifying p'. This leads to the simplified relations $xy = (Q^2 + M^2)/S$, $z = 1$, $M_{X'} = 0$, $\hat{s} = M^2$, $\hat{t} = 0$, $\hat{u} = -Q^2$, $p_T^\star = 0$, $y_H^\star = \ln(W/M)$, $p_T = \sqrt{(1-y)Q^2}$, $y_H = \ln(yS/mm_T)$, and $\cos\phi = -1$. As before, we have $W^2 = yS - Q^2$. In turn, Q^2 and x may be expressed in terms of p_T and y_H, as

$$Q^2 = \frac{p_T^2}{1 - m m_T \exp(y_H)/S}, \qquad x = \frac{m_T \exp(-y_H)/m - M^2/S}{1 - m m_T \exp(y_H)/S}, \tag{26}$$

which allows us to conveniently evaluate the p_T and y_H distributions from Eq. (25).

In the remainder of this section, we recall the analysis [15,16] of the total cross section of $\nu + N \to \nu + H + N'$, with $H = J/\psi, \chi_{c1}, \psi'$, in diffractive DIS. We first consider the case $H = J/\psi$. The differential cross section of $\nu + N \to \nu + H + N'$ may be be obtained from the one of $\mu + N \to \mu + H + N'$ in diffractive DIS via a virtual photon $\gamma^\star$ by adjusting the electroweak couplings and the propagator, as

$$\frac{d^2\sigma}{dy\,dQ^2}(\nu + N \to \nu + H + N') = \left[\frac{g^2 v_c Q^2}{e^2 e_c\,(Q^2 + M_Z^2)}\right]^2 \frac{d^2\sigma}{dy\,dQ^2}(\mu + N \to \mu + H + N'). \quad (27)$$

The latter can be decomposed as [26]

$$\frac{d^2\sigma}{dy\,dQ^2}(\mu + N \to \mu + H + N') = \frac{\alpha}{2\pi}\,\frac{y - Q^2/(2Em)}{Q^2(y^2 + Q^2/E^2)}\left\{\left[1 + (1-y)^2 + \frac{Q^2}{2E^2}\right]\sigma_T(\nu, Q^2) + \left[2(1-y) - \frac{Q^2}{2E^2}\right]\sigma_L(\nu, Q^2)\right\}, \quad (28)$$

where $\sigma_T(\nu, Q^2)$ and $\sigma_L(\nu, Q^2)$ are the transverse and longitudinal parts of the diffractive cross section of $\gamma^\star + N \to H + N'$ in virtual photoproduction, respectively. Here, $E = (S - m^2)/(2m)$ and $\nu = q \cdot P/m = yE = q^0$ are the incoming-lepton and virtual-photon energies in the nucleon rest frame, respectively, $\sqrt{S}$ is the lepton-nucleon CM energy, and the muon mass is neglected. At small values of Q^2, the contribution from longitudinal photons is suppressed, and we may put $\sigma_L(\nu, Q^2) = 0$. On the other hand, according to the VDM, the Q^2 dependence of $\sigma_T(\nu, Q^2)$ is approximately described by the familiar dipole suppression factor, viz.

$$\sigma_T(\nu, Q^2) = \frac{\sigma(\nu)}{(1 + Q^2/M_V^2)^2}, \quad (29)$$

where $\sigma(\nu)$ is the diffractive cross section of $\gamma + N \to H + N'$ in real photoproduction and M_V is a phenomenological mass parameter. Fits to experimental data of $\gamma^\star + N \to H + N'$ suggest that $M_V = (3.2 \pm 0.6)$ GeV [27]. The measured ν dependence of $\sigma(\nu)$ is well described by the phenomenological parameterization [15,16,28,29,30]

$$\sigma(\nu) = A \exp\frac{-B}{\nu - C}, \quad (30)$$

with $A = 20$ nb, $B = 45$ GeV, and $C = 6$ GeV [30], which is valid for $\nu > C$.

We now generalize our considerations to also include the cases $H = \chi_{c1}, \psi'$. To this end, we recall that the strengths of the Z-boson vector and axial-vector couplings to the S- and P-wave charmonia are proportional to $v_c f_V$ and $a_c f_A$, where [16]

$$f_V^2 = \frac{3}{8\pi}\,\frac{|R_S(0)|^2}{m_c^3},$$
$$f_A^2 = \frac{9}{4\pi}\,\frac{|R'_P(0)|^2}{m_c^5}, \quad (31)$$

respectively. Here, $R_S(r)$ and $R_P(r)$ denote the radial wave functions of the S- and P-wave charmonia, respectively. Furthermore, we have [1]

$$|R_S(0)|^2 = \frac{2\pi}{9} \left\langle \mathcal{O}^{\psi} \left[{}^3S_1^{(1)} \right] \right\rangle$$
$$|R'_P(0)|^2 = \frac{2\pi}{9} \frac{\left\langle \mathcal{O}^{\chi_{cJ}} \left[{}^3P_J^{(1)} \right] \right\rangle}{2J+1}. \tag{32}$$

Assuming that $\sigma(\psi' + N \to \psi' + N') \approx \sigma(\chi_{c1} + N \to \chi_{c1} + N') \approx \sigma(J/\psi + N \to J/\psi + N')$, we thus conclude that $d^2\sigma(\nu + N \to \nu + \psi' + N')/(dy\, dQ^2)$ and $d^2\sigma(\nu + N \to \nu + \chi_{c1} + N')/(dy\, dQ^2)$ may be obtained from $d^2\sigma(\nu + N \to \nu + J/\psi + N')/(dy\, dQ^2)$ through multiplication with the constant factors

$$R_{\psi'} = \frac{\left\langle \mathcal{O}^{\psi'} \left[{}^3S_1^{(1)} \right] \right\rangle}{\left\langle \mathcal{O}^{J/\psi} \left[{}^3S_1^{(1)} \right] \right\rangle},$$
$$R_{\chi_{c1}} = \frac{a_c^2}{v_c^2} \frac{6}{m_c^2} \frac{\left\langle \mathcal{O}^{\chi_{c0}} \left[{}^3P_0^{(1)} \right] \right\rangle}{\left\langle \mathcal{O}^{J/\psi} \left[{}^3S_1^{(1)} \right] \right\rangle}, \tag{33}$$

respectively. Thus, the effective direct-to-prompt conversion factor reads

$$R_{(J/\psi)_{\rm prompt}} = 1 + R_{\chi_{c1}} B(\chi_{c1} \to J/\psi + \gamma) + R_{\psi'} B(\psi' \to J/\psi + X). \tag{34}$$

The kinematically allowed ranges of E, Q^2, and y are

$$E > M\left(1 + \frac{M}{2m}\right),$$
$$0 < Q^2 < \frac{2E[2Em - M(M+2m)]}{2E+m},$$
$$\frac{Q^2 + M(M+2m)}{2Em} < y < 1 - \frac{Q^2}{4E^2}, \tag{35}$$

respectively. Here, the N' mass is taken to be m. In addition, Eq. (30) implies the cut $y > C/E$.

3 Numerical results

We are now in a position to present our numerical results. We first describe our theoretical input and the kinematic conditions. We use $m = 0.938$ GeV, $m_c = (1.5 \pm 0.1)$ GeV [21], $M_V = (3.2 \pm 0.6)$ GeV [27], $M_W = 80.419$ GeV, $M_Z = 91.1882$ GeV, $\sin^2\theta_w = 1 - M_W^2/M_Z^2 = 0.22225$, $G_F = 1.16639 \times 10^{-5}$ GeV^{-2}, $\alpha = 1/137.036$, and the LO formula for $\alpha_s^{(n_f)}(\mu)$ with $n_f = 3$ active quark flavours [21]. The CHORUS Collaboration [12] chose the target material to be lead (Pb), which in average consists of $A = 207.2$ nucleons, $Z = 82$ of them being protons. The NOMAD Collaboration [13] uses iron

(Fe), with $A = 55.854$ and $Z = 26$. Leaving aside nuclear corrections and appealing to strong-isospin symmetry, the effective nucleon PDFs may be approximated by

$$f_{a/N}(x,\mu_f) = \frac{1}{A}\left[Z f_{a/p}(x,\mu_f) + (A-Z) f_{b/p}(x,\mu_f)\right],$$
$$f_{c/N}(x,\mu_f) = f_{c/p}(x,\mu_f), \tag{36}$$

where $(a,b) = (u,d), (\overline{u},\overline{d}), (d,u), (\overline{d},\overline{u})$ and $c = s, \overline{s}, g$. We present the cross sections per nucleon, rather than per nucleus. The dependence of the cross section per nucleus, σ_A, on the number of nucleons, A, was studied experimentally for J/ψ inclusive photoproduction [31,32] and muoproduction [33,34]. The New Muon Collaboration (NMC) [34], who performed the most recent of these experiments, was able to reconcile the seemingly inconsistent results of the previous experiments [31,32,33] by imposing appropriate cuts on z and p_T. Separating signal events of elastic (coherent) and deep-inelastic (incoherent) scattering, the A dependences of the respective cross sections σ_A were found to differ significantly [32,34]. Assuming that σ_A is related to the cross section per free nucleon (hydrogen), σ_1, by the simple power law $\sigma_A = A^\alpha \sigma_1$ [32,35], with α being an A-independent number, we extract the values $\alpha_{\rm coh} = 1.19 \pm 0.02$ and $\alpha_{\rm in} = 1.05 \pm 0.03$ from the NMC results for coherent and incoherent scattering, respectively. For lead (iron) targets, this implies that the elastic and deep-inelastic cross sections per (bound) nucleon, σ_A/A, are enhanced relative to the respective values of σ_1 by factors of $2.75^{+0.32}_{-0.27}$ ($2.15^{+0.18}_{-0.17}$) and $1.31^{+0.22}_{-0.20}$ ($1.22^{+0.16}_{-0.14}$), respectively. We note in passing that the above value of $\alpha_{\rm in}$ is in same ball park as those recently found for inclusive large-p_T prompt-photon and neutral-pion hadroproduction in fixed-target scattering, namely 1.04 and 1.08, respectively [35]. We assume that the power laws of J/ψ muoproduction, which dominantly proceeds via the electromagnetic current, carry over to νN NC DIS and employ them to determine the nuclear corrections. As for the proton PDFs, we employ the LO set by Martin, Roberts, Stirling, and Thorne (MRST98LO) [36], with asymptotic scale parameter $\Lambda^{(4)} = 174$ MeV, as our default and the LO set by the CTEQ Collaboration (CTEQ5L) [37], with $\Lambda^{(4)} = 192$ MeV, for comparison. The corresponding values of $\Lambda^{(3)}$ are 204 MeV and 224 MeV, respectively. We choose the renormalization and factorization scales to be $\mu_i = \xi_i \sqrt{Q^2 + M^2}$, with $i = r, f$, respectively, and independently vary the scale parameters ξ_r and ξ_f between 1/2 and 2 about the default value 1. We adopt the NRQCD MEs from Table I of Ref. [7], which were determined there from the measured leptonic annihilation rates of the J/ψ and ψ' mesons and fits to the Tevatron data [4]. As for the J/ψ and ψ' mesons, the fit results for $\left\langle \mathcal{O}^\psi \left[{}^1S_0^{(8)}\right]\right\rangle$ and $\left\langle \mathcal{O}^\psi \left[{}^3P_0^{(8)}\right]\right\rangle$ are strongly correlated, so that the linear combinations

$$M_r^\psi = \left\langle \mathcal{O}^\psi \left[{}^1S_0^{(8)}\right]\right\rangle + \frac{r}{m_c^2}\left\langle \mathcal{O}^\psi \left[{}^3P_0^{(8)}\right]\right\rangle, \tag{37}$$

with suitable values of r, are quoted. Since Eq. (13) is sensitive to different linear combinations of $\left\langle \mathcal{O}^\psi \left[{}^1S_0^{(8)}\right]\right\rangle$ and $\left\langle \mathcal{O}^\psi \left[{}^3P_0^{(8)}\right]\right\rangle$ than appear in Eq. (37), we write $\left\langle \mathcal{O}^\psi \left[{}^1S_0^{(8)}\right]\right\rangle = \kappa_\psi M_r^\psi$ and $\left\langle \mathcal{O}^\psi \left[{}^3P_0^{(8)}\right]\right\rangle = (1-\kappa_\psi)\,(m_c^2/r)\,M_r^\psi$ and independently vary $\kappa_{J/\psi}$ and $\kappa_{\psi'}$ between 0 and 1 around the default value 1/2. The wide-band neutrino beam utilized in the

CHORUS and NOMAD experiments mainly consists of ν_μ neutrinos and contains $\overline{\nu}_\mu$, ν_e, and $\overline{\nu}_e$ admixtures of about 6%, 1%, and below 1%, respectively. The average ν_μ energy is 27 GeV. Using accurate parameterizations for the energy spectra $\phi_\nu(E_\nu)$ of the individual neutrino species ν [13], we calculate the spectrum-averaged cross section as

$$\sigma = \frac{\sum_\nu \int dE_\nu \, \phi_\nu(E_\nu) \sigma_\nu(E_\nu)}{\sum_\nu \int dE_\nu \, \phi_\nu(E_\nu)}, \tag{38}$$

where $\nu = \nu_e, \overline{\nu}_e, \nu_\mu, \overline{\nu}_\mu$. In order to conform with the CHORUS analysis, we apply the acceptance cut $20 < E_\nu < 200$ GeV.

In order to estimate the theoretical uncertainties in our predictions, we vary the unphysical parameters ξ_r, ξ_f, $\kappa_{J/\psi}$, and $\kappa_{\psi'}$ as indicated above, take into account the experimental errors on $\alpha_{\rm coh}$, $\alpha_{\rm in}$, m_c, M_V, the relevant charmonium decay branching fractions, and the default MEs, and switch from our default PDF set to the CTEQ5L one, properly adjusting $\Lambda^{(3)}$ and the MEs. We then combine the individual shifts in quadrature, allowing for the upper and lower half-errors to be different.

In Figs. 3 and 4, we respectively present the p_T and $y_{J/\psi}$ distributions of prompt J/ψ production in nondiffractive νN NC DIS under CHORUS experimental conditions predicted to LO in NRQCD. Specifically, the $2 \to 2$ CO contributions (upper histograms) are compared with the $2 \to 3$ CS ones (lower histograms). In each case, the theoretical errors, evaluated as explained above, are indicated by the hatched areas. Since the contributing partonic cross sections are all gluon initiated, our our central predictions can be rendered appropriate for NOMAD by simply adjusting the nuclear correction factor, by multiplication with 0.94. We observe that the shapes of the CO and CS distributions are very similar. However, the CO distributions greatly exceed the CS ones in normalization. In fact, the integrated CO and CS cross sections are $3.0^{+1.6}_{-1.7} \times 10^{-3}$ fb and $1.0^{+0.7}_{-0.5} \times 10^{-4}$ fb, respectively, the ratio of the central values being 30. The bulk parts, 72% in the CO case and 78% in the CS case, are due to direct J/ψ production. In the first case, the fractions due to feed-down from χ_{cJ} and ψ' mesons are each 14%, while, in the CS case, there is only feed down from ψ' mesons. Therefore, at first sight, the suppression of the CSM prediction seems to contradict the naïve expectation based on the NRQCD counting rules (see Table 1). However, detailed inspection reveals that this suppression can be attributed to the smallness of the effective value of $\sqrt{S}$, which affects the $2 \to 3$ phase space of the CS process more severely than the $2 \to 2$ one of the CO processes. For $E = 27$ GeV, we just have $\sqrt{S} = 7.2$ GeV. For a monoenergetic neutrino beam with $E = 48$ TeV, so that $\sqrt{S} = 300$ GeV as for ep collisions at DESY HERA, the CO to CS ratio becomes 4.5. This should be compared with the corresponding analysis for direct J/ψ production in nondiffractive ep DIS at HERA, with $Q^2 > 4$ GeV^2, which yields a CO to CS ratio of 7.8 [22].

We find the total cross section of prompt J/ψ production in diffractive νN NC DIS to be $3.3^{+1.6}_{-1.4} \times 10^{-3}$ fb. The theoretical uncertainty quoted here is merely parametric; it neither includes the experimental error on $\sigma(\nu)$ as parameterized by Eq. (30), nor does it reflect the unavoidable lack of rigour of the underlying model assumptions. The fractions due to feed-down from χ_{c1} and ψ' mesons amount to 19% and 17%, respectively. The

corresponding prediction for NOMAD is obtained through multiplication with the scaling factor 0.80, which accounts for the difference in the nuclear correction factor.

The CHORUS Collaboration measured the spectrum-averaged total cross section per nucleon of $\nu + N \to \nu + J/\psi + X$ in DIS to be $(6.3 \pm 3.0) \times 10^{-2}$ fb. In Fig. 5, this experimental data point is shown together with our theoretical predictions for the CO, CS, and diffractive contributions. It should be compared with their sum, 6.4×10^{-3} fb. As for the central values, the measurement exceeds the combined prediction by a factor of 10. We have to bear in mind that our theoretical prediction for the nondiffractive cross section is of LO in α_s and v. The NLO corrections are expected to lead to a substantial enhancement. It would be desirable if the CHORUS Collaboration were able to substantially increase their data sample and to exclude the diffractive regime by imposing suitable acceptance cuts on z, $p_T^\star$, or $M_{X'}$, and if the NOMAD and NuTeV Collaborations could come up with similar measurements.

4 Conclusions

We provided, in analytic form, the cross sections of the partonic subprocesses $\nu + a \to \nu + c\overline{c}[n] + a$, where $a = q, \overline{q}, g$ and $n = {}^3S_1^{(1)}, {}^3P_J^{(1)}, {}^1S_0^{(8)}, {}^3S_1^{(8)}, {}^3P_J^{(8)}$, to LO in the NRQCD factorization formalism [1]. We also confirmed previous results for the cross sections of the partonic subprocesses $\nu + g \to \nu + c\overline{c}[n]$, where $n = {}^1S_0^{(8)}, {}^3S_1^{(8)}, {}^3P_J^{(8)}$ [23]. Using these results, we then studied the cross section of prompt J/ψ inclusive production in nondiffractive νN NC DIS to LO in NRQCD and the CSM. We presented the cross section per nucleon bound in lead and averaged it over the effective energy spectrum of the wide-band neutrino beam employed in the CHORUS [12] and NOMAD [13] experiments. Apart from the total cross section, we also considered the p_T and $y_{J/\psi}$ distributions. The cross sections of the $2 \to 3$ CO partonic subprocesses, which did not enter our phenomenological study, can be used in the future, at LO, in connection with an appropriate acceptance cut on z, $p_T^\star$, or $M_{X'}$ to exclude the collinear singularities in the limit $\hat{t} \to 0$ or, at NLO, as an essential ingredient for the real radiative corrections to the inclusive cross section of $\nu + N \to \nu + J/\psi + X$. A similar comment applies to the $2 \to 3$ CS partonic subprocesses of χ_{cJ} production, where the singularities are of IR type. Repeating the analysis of Refs. [15,16] with up-to-date input, we also evaluated the total cross section of prompt J/ψ inclusive production in diffractive νN NC DIS.

As for nondiffractive direct J/ψ production, from the NRQCD counting rules, one expects the CO contribution, which arises from $2 \to 2$ partonic subprocesses, to be slightly suppressed, by a factor of $v^4/\alpha_s \approx \alpha_s$ relative to the CS one, which is generated by $2 \to 3$ partonic subprocesses. However, our analysis revealed that, under CHORUS kinematic conditions, the CS contribution is approximately 30 times smaller than the CO one. We demonstrated that this may be attributed to the smallness of the effective value of $\sqrt{S}$, which constrains the $2 \to 3$ phase space more severely than the $2 \to 2$ one.

As far as central values are concerned, the CHORUS measurement of the spectrum-averaged total cross section per nucleon of $\nu + N \to \nu + J/\psi + X$ in DIS overshoots our

combined prediction by a factor of 10. However, this comparison does not yet permit any meaningful conclusions concerning the validity of the NRQCD factorization formalism [1]. On the one hand, our theoretical prediction for the nondiffractive contribution should be substantially increased by the inclusion of NLO corrections, which are presently still unknown. On the other hand, the experimental error is still rather sizeable, and the diffractive events have not been separated from the experimental data set.

Acknowledgements

We are indebted to Maarten de Jong and Lalit Sehgal for useful communications concerning Refs. [30] and [20], respectively, and to Kai Zuber for providing us with the energy spectra of the CERN wide-band neutrino beam in numerical form and for helpful discussions regarding Ref. [13]. The work of L.Z. was supported by the Studienstiftung des deutschen Volkes through a PhD scholarship. This work was supported in part by the Deutsche Forschungsgemeinschaft through Grant No. KN 365/1-1, by the Bundesministerium für Bildung und Forschung through Grant No. 05 HT1GUA 4, by the European Commission through the Research Training Network *Quantum Chromodynamics and the Deep Structure of Elementary Particles* under Contract No. ERBFMRX-CT98-0194, and by Sun Microsystems through Academic Equipment Grant No. EDUD-7832-000332-GER.

A Partonic cross sections

In this Appendix, we present analytic expressions for the coefficients $F_a[n]$, $T_a[n]$, $L_a[n]$, and $A_a[n]$ appearing in Eq. (12). In order to compactify the expressions, it is useful to introduce the Lorentz invariants $s = 2q\cdot p$, $t = -2p\cdot p'$, and $u = -2q\cdot p'$, which are related to the partonic Mandelstam variables by $s = \hat{s} + Q^2$, $t = \hat{t}$, and $u = \hat{u} + Q^2$, respectively.

$\nu(\overline{\nu}) + q(\overline{q}) \to \nu(\overline{\nu}) + c\overline{c}\left[{}^3S_1^{(1)}\right] + q(\overline{q})$:

$$F = T = L = A = 0. \tag{A.1}$$

$\nu(\overline{\nu}) + q(\overline{q}) \to \nu(\overline{\nu}) + c\overline{c}\left[{}^3P_J^{(1)}\right] + q(\overline{q})$:

$$F = T = L = A = 0. \tag{A.2}$$

$\nu(\overline{\nu}) + q(\overline{q}) \to \nu(\overline{\nu}) + c\overline{c}\left[{}^1S_0^{(8)}\right] + q(\overline{q})$:

$$\begin{aligned} F &= \frac{-g^4\alpha_s^2 v_c^2 Q^2}{6\pi M (Q^2+M_Z^2)^2 s^4 t (s+u)^2}, \\ T &= 2Q^4t^2 + 2Q^2st(s+u) + s^4 + s^2u^2, \\ L &= -2Q^2t(Q^2t+su), \\ A &= 0. \end{aligned} \tag{A.3}$$

$\nu(\overline{\nu}) + q(\overline{q}) \to \nu(\overline{\nu}) + c\overline{c}\left[{}^3S_1^{(8)}\right] + q(\overline{q})$:

$$
\begin{aligned}
F &= \frac{g^4\alpha_s^2}{36\pi M^3(Q^2+M_Z^2)^2(Q^2-s)^2(Q^2-u)^2s^4t(s+u)^2},\\
T &= -(a_q^2+v_q^2)Q^2t(s+u)^2\{2Q^6t^2(2s+t)+2Q^4s[s^2u-st(3t-2u)-2t^3]+Q^2s^2[s^2(t\\
&\quad -2u)+2s(t^2-4tu-u^2)+t(2t^2-2tu-u^2)]+s^3u(s^2+2st+2t^2+2tu+u^2)\}\\
&\quad +4a_qa_cQ^2t(s+u)(Q^2-s)(Q^2-u)\{Q^6t(s+2t)+Q^4[s^3-s^2(t-2u)-5st^2-2t^2(t\\
&\quad +u)]-Q^2s[s^3+s^2(t+5u)-s(2t^2-5tu-3u^2)-t(2t^2+tu-u^2)]+s^2u[2s^2+s(4t\\
&\quad +3u)+2t^2+3tu+u^2]\}-2a_c^2Q^2(Q^2-s)^2(Q^2-u)^2\{2Q^6t^2+2Q^4t[s^2-s(3t-u)-3t(t\\
&\quad +u)]-Q^2[s^4+6s^3t+s^2(2t^2+12tu+u^2)-2st(4t^2+tu-3u^2)-4t^2(t+u)^2]+s^5\\
&\quad +s^4(5t+u)+s^3(8t^2+12tu+u^2)+s^2(4t^3+16t^2u+13tu^2+u^3)+4stu(t+u)^2\},\\
L &= 2(a_q^2+v_q^2)Q^4(Q^2-s)^2t^2(s+t)^2(s+u)^2-4a_qa_cQ^2(Q^2-s)^2(Q^2-u)t(s+u)[Q^4t(s\\
&\quad +2t)-Q^2(s^3+2s^2t+3st^2+2t^3+2t^2u)+s^4+s^3(2t+u)+s^2t^2-stu(t+u)]+2a_c^2(Q^2\\
&\quad -s)^2(Q^2-u)^2\{2Q^8t^2-2Q^6t[s^2+s(3t-u)+3t(t+u)]+Q^4[s^4+4s^3t+s^2(8t^2-2tu\\
&\quad +u^2)+2st(4t^2+tu-3u^2)+4t^2(t+u)^2]-2Q^2s[s^4+s^3(2t+u)+s^2(2t^2+u^2)+s(t^3\\
&\quad -2t^2u-2tu^2+u^3)-2tu(t+u)^2]+s^2(s+t+u)^2(s^2+u^2)\},\\
A &= \pm 2v_qQ^2st(s+u)\{a_q(s+u)[2Q^6st-2Q^4t(2s^2+st-tu)\\
&\quad +Q^2s(s^2(t-2u)+2s(t^2+u^2)-tu(2t-u))+s^2u(s-u)(s+2t+u)]\\
&\quad -2a_c(Q^2-s)(Q^2-u)[Q^6t-Q^4(s^2+3st+t^2)\\
&\quad +Q^2(s^3+s^2(3t+u)+s(2t^2+tu+u^2)-tu(t+u))-su^2(s+t+u)]\},
\end{aligned}
\tag{A.4}
$$

where the plus (minus) sign refers to a $\nu+q$ or $\overline{\nu}+\overline{q}$ ($\nu+\overline{q}$ or $\overline{\nu}+q$) initial state.

$\nu(\overline{\nu}) + q(\overline{q}) \to \nu(\overline{\nu}) + c\overline{c}\left[{}^3P_J^{(8)}\right] + q(\overline{q})$:

$$
\begin{aligned}
F &= \frac{2g^4\alpha_s^2v_c^2Q^2}{3\pi M^3(Q^2+M_Z^2)^2s^4t(s+u)^4},\\
T &= 8Q^6t[2s^2+st+t(2t+u)]-2Q^4[4s^4+12s^3t+s^2(19t^2+8tu+4u^2)+2st(6t^2\\
&\quad +tu-2u^2)+t^2(8t^2+12tu+7u^2)]+2Q^2s[6s^4+s^3(7t+6u)+s^2(4t^2+3tu\\
&\quad +6u^2)-su(8t^2+3tu-6u^2)-tu(8t^2+12tu+7u^2)]-s^2(s+u)[7s^3+s^2(12t\\
&\quad +7u)+s(8t^2+16tu+7u^2)+u(8t^2+12tu+7u^2)],\\
L &= 8Q^6t[s^2-st-t(2t+u)]-2Q^4[2s^4+4s^3t+s^2(5t^2+8tu+2u^2)-2st(6t^2\\
&\quad +tu-2u^2)-t^2(8t^2+12tu+7u^2)]+2Q^2s(s+u)[2s^3+2s^2t+s(8t^2+5tu\\
&\quad +2u^2)+t(8t^2+12tu+7u^2)],\\
A &= 0.
\end{aligned}
\tag{A.5}
$$

$\nu(\overline{\nu}) + g \to \nu(\overline{\nu}) + c\overline{c}\left[{}^3S_1^{(1)}\right] + g$:

$$
F = \frac{-2g^4\alpha_s^2v_c^2Q^2}{27\pi M(Q^2+M_Z^2)^2s^4(s+t)^2(s+u)^2(t+u)^2},
$$

$$
\begin{aligned}
T &= 4Q^6t^2(s^2+t^2) - 2Q^4t[s^3(3t-2u) + 3s^2t(t+u) + 2st^2(t-u) + 2t^3(t+u)] \\
&\quad + 2Q^2s[s^3(t-u)^2 - 2s^2tu(t+u) - st^2u(2t-u) - 2t^3u(t+u)] - 2s^2[s^3(t^2 \\
&\quad + tu+u^2) + s^2(t+u)^3 + stu(t^2+3tu+u^2) + t^2u^2(t+u)], \\
L &= 2Q^6t^2(s^2-2t^2) - 2Q^4t(s^2-2t^2)[s(t-u) + t(t+u)] + Q^2s[s^3(t^2+u^2) \\
&\quad + 2s^2t^2(t+u) + st^2(t^2+6tu+u^2) + 4t^3u(t+u)], \\
A &= 0.
\end{aligned} \tag{A.6}
$$

$\nu(\overline{\nu}) + g \to \nu(\overline{\nu}) + c\overline{c}\left[{}^3P_0^{(1)}\right] + g$:

$$
\begin{aligned}
F &= \frac{8g^4\alpha_s^2a_c^2(Q^2+M^2)^2}{27\pi M^3(Q^2+M_Z^2)^2s^4(s+t)^4(s+u)^4(t+u)^4}, \\
T &= 4Q^8t^2[s^6 - 2s^4u^2 + s^3(t^3-tu^2) + s^2(2t^4+4t^3u+2t^2u^2+u^4) + st(2t^4+6t^3u+5t^2u^2 \\
&\quad +2tu^3+u^4) + t^2(t+u)^2(t^2+u^2)] - 4Q^6t[s^7(2t-u) + s^6t(t+u) - 2s^5(t^3+t^2u+2tu^2 \\
&\quad -u^3) - s^4t(t^3+6t^2u+7tu^2+2u^3) + s^3(t^5-3t^4u-7t^3u^2-3t^2u^3+2tu^4-u^5) + s^2t(t^5 \\
&\quad +4t^4u+3t^3u^2+2t^2u^3+3tu^4+u^5) + st^2u(t+u)^2(2t^2+5tu+u^2) + 2t^3u^2(t+u)^3] \\
&\quad +2Q^4t[2s^8(t-2u) + 2s^7(t^2-u^2) - s^6(3t^3-2t^2u-tu^2-8u^3) - 2s^5(2t^4+4t^3u+t^2u^2 \\
&\quad -4tu^3-3u^4) + s^4(t^5-6t^4u-6t^3u^2+2t^2u^3+3tu^4-4u^5) + 2s^3(t+u)^2(2t^4+2t^3u \\
&\quad -t^2u^2+tu^3-2u^4) + s^2t(t+u)^2(2t^4+12t^3u+9t^2u^2-4tu^3-2u^4) + 2st^2u(t+u)^3(2t^2 \\
&\quad +4tu-u^2) + 2t^3u^2(t+u)^4] + 2Q^2stu[2s^8 + 2s^7(t+u) - s^6(3t^2+2tu+3u^2) - 2s^5(2t^3 \\
&\quad +5t^2u+6tu^2+3u^3) + s^4(t^4-4t^3u-8t^2u^2-4tu^3+u^4) + 2s^3(2t^5+7t^4u+11t^3u^2 \\
&\quad +10t^2u^3+6tu^4+2u^5) + s^2(t+u)^2(2t^4+12t^3u+15t^2u^2+6tu^3+2u^4) + 2stu(t+u)^3(2t^2 \\
&\quad +4tu+u^2) + 2t^2u^2(t+u)^4], \\
L &= -2Q^8t^2[s^6 - 2s^4u^2 + 2s^3(t^3-tu^2) + s^2(4t^4+8t^3u+4t^2u^2+u^4) + 2st(2t^4+6t^3u+5t^2u^2 \\
&\quad +2tu^3+u^4) + 2t^2(t+u)^2(t^2+u^2)] + 2Q^6t[s^7(3t-u) + 3s^6t(t+u) - 2s^5(2t^3+3t^2u \\
&\quad +4tu^2-u^3) - 2s^4t(t^3+8t^2u+9tu^2+2u^3) + s^3(6t^5-2t^4u-18t^3u^2-8t^2u^3+5tu^4-u^5) \\
&\quad +s^2t(4t^5+12t^4u+6t^3u^2+4t^2u^3+7tu^4+u^5) + 2st^2u(t+u)^2(2t^2+5tu+u^2) + 4t^3u^2(t \\
&\quad +u)^3] - Q^4[s^8(7t^2-4tu+u^2) + 2s^7t(7t^2+5tu-2u^2) - s^6(5t^4-6t^3u-t^2u^2-12tu^3 \\
&\quad +2u^4) - 8s^5t(3t-u)(t+u)^3 - s^4(8t^6+76t^5u+110t^4u^2+40t^3u^3-5t^2u^4+8tu^5-u^6) \\
&\quad +2s^3t(4t^6+2t^5u-22t^4u^2-22t^3u^3-t^2u^4-tu^5-2u^6) + s^2t^2(t+u)^2(4t^4+24t^3u+8t^2u^2 \\
&\quad -4tu^3-u^4) + 4st^3u(t+u)^3(2t^2+4tu-u^2) + 4t^4u^2(t+u)^4] + 2Q^2s(s+u)[s^7(2t^2-tu \\
&\quad +u^2) + 2s^6t^2(3t+u) + s^5(4t^4+9t^3u+6t^2u^2+3tu^3-2u^4) - s^4t(4t^4-11t^2u^2-12tu^3 \\
&\quad -u^4) - s^3(6t^6+18t^5u+12t^4u^2-t^3u^3+2t^2u^4+2tu^5-u^6) - s^2t(t+u)^2(2t^4+12t^3u \\
&\quad +6t^2u^2+2tu^3+u^4) - 2st^3u(t+u)^3(2t+3u) - 2t^3u^2(t+u)^4] - s^2(s+u)^2(s+t+u)^2[s^4 \\
&\quad (t^2+u^2) + 2s^3(t^3-u^3) + s^2(t^4+2t^3u+2t^2u^2+u^4) + 2st^3u(t+u) + t^2u^2(t+u)^2], \\
A &= 0.
\end{aligned} \tag{A.7}
$$

$\nu(\overline{\nu}) + g \to \nu(\overline{\nu}) + c\overline{c}\left[{}^3P_1^{(1)}\right] + g$:

$$F = \frac{4g^4\alpha_s^2 a_c^2}{27\pi M^3(Q^2+M_Z^2)^2 s^4(s+t)^4(s+u)^4(t+u)^4},$$

$$\begin{aligned}
T = &-8Q^{10}t^4(s+t)(t+u)[3s^3+s^2(7t+10u)+s(5t^2+15tu+9u^2)+t^3+5t^2u+7tu^2\\
&+2u^3]-4Q^8t^2[s^8+7s^7(t+u)+s^6(24t^2+48tu+22u^2)+2s^5(17t^3+62t^2u+60tu^2\\
&+15u^3)+s^4(7t^4+112t^3u+219t^2u^2+130tu^3+17u^4)-s^3(30t^5+37t^4u-91t^3u^2\\
&-151t^2u^3-56tu^4-3u^5)-s^2t(t+u)^2(31t^3+62t^2u-18tu^2-4u^3)-st(11t^6+69t^5u\\
&+144t^4u^2+123t^3u^3+42t^2u^4+6tu^5+u^6)-t^3(t+u)^2(t^3+9t^2u+17tu^2+7u^3)]\\
&+2Q^6t[s^9(4t-2u)+2s^8(16t^2+9tu-7u^2)+s^7(125t^3+206t^2u+25tu^2-44u^3)\\
&+s^6(239t^4+695t^3u+507t^2u^2-9tu^3-60u^4)+s^5(221t^5+1022t^4u+1410t^3u^2\\
&+602t^2u^3-35tu^4-34u^5)+s^4(91t^6+689t^5u+1548t^4u^2+1318t^3u^3+361t^2u^4\\
&-13tu^5-6u^6)+s^3t(t+u)^2(16t^4+156t^3u+357t^2u^2+78tu^3+2u^4)+s^2t^2(10t^6\\
&+24t^5u+57t^4u^2+127t^3u^3+99t^2u^4-tu^5-16u^6)+2st^2(t+u)^2(4t^5+2t^4u\\
&-17t^3u^2-19t^2u^3-12tu^4-4u^5)+2t^3(t+u)^4(t^3-4tu^2-u^3)]-2Q^4[s^{10}(3t^2\\
&-2tu+u^2)+s^9(25t^3+7t^2u-11tu^2+7u^3)+s^8(100t^4+132t^3u-25t^2u^2-22tu^3\\
&+23u^4)+s^7(208t^5+539t^4u+277t^3u^2-93t^2u^3-5tu^4+34u^5)+s^6(217t^6\\
&+935t^5u+1162t^4u^2+366t^3u^3-66t^2u^4+29tu^5+23u^6)+s^5(87t^7+688t^6u\\
&+1545t^5u^2+1320t^4u^3+406t^3u^4+59t^2u^5+36tu^6+7u^7)-s^4(t+u)^2(22t^6-119t^5u\\
&-396t^4u^2-184t^3u^3-72t^2u^4-17tu^5-u^6)-s^3t(28t^8+152t^7u+257t^6u^2+100t^5u^3\\
&-163t^4u^4-241t^3u^5-158t^2u^6-51tu^7-4u^8)-s^2t^2(t+u)^2(6t^6+52t^5u+132t^4u^2\\
&+125t^3u^3+47t^2u^4-5tu^5-7u^6)-2st^3u(t+u)^4(3t^3+12t^2u+8tu^2+2u^3)-2t^4u^2(t\\
&+u)^6]+2Q^2s[s^{10}(t^2+u^2)+s^9(8t^3+6t^2u+6tu^2+8u^3)+s^8(32t^4+56t^3u+42t^2u^2\\
&+52tu^3+30u^4)+s^7(75t^5+232t^4u+261t^3u^2+221t^2u^3+174tu^4+57u^5)+s^6(105t^6\\
&+508t^5u+888t^4u^2+836t^3u^3+576t^2u^4+280tu^5+57u^6)+2s^5(43t^7+308t^6u+791t^5u^2\\
&+1015t^4u^3+774t^3u^4+389t^2u^5+119tu^6+15u^7)+s^4(t+u)^2(38t^6+332t^5u+799t^4u^2\\
&+754t^3u^3+389t^2u^4+96tu^5+8u^6)+s^3(7t^9+134t^8u+734t^7u^2+1847t^6u^3+2546t^5u^4\\
&+2066t^4u^5+993t^3u^6+262t^2u^7+30tu^8+u^9)+2s^2tu(t+u)^2(8t^6+65t^5u+167t^4u^2\\
&+193t^3u^3+111t^2u^4+29tu^5+2u^6)+st^2u^2(t+u)^4(11t^3+34t^2u+28tu^2+7u^3)\\
&+2t^3u^3(t+u)^6],
\end{aligned}$$

$$\begin{aligned}
L = &\,8Q^{10}t^4(s+t)(t+u)[3s^3+s^2(7t+10u)+s(5t^2+15tu+9u^2)+t^3+5t^2u+7tu^2+2u^3]\\
&+2Q^8t^2[s^8-2s^7(t+u)-s^6(21t^2+42tu+23u^2)-2s^5(29t^3+62t^2u+55tu^2+22u^3)\\
&-s^4(98t^4+218t^3u+176t^2u^2+90tu^3+33u^4)-2s^3(54t^5+157t^4u+130t^3u^2+35t^2u^3\\
&+13tu^4+5u^5)-s^2(t+u)^2(70t^4+156t^3u+4t^2u^2+6tu^3+u^4)-2st(11t^6+69t^5u\\
&+144t^4u^2+123t^3u^3+42t^2u^4+6tu^5+u^6)-2t^3(t+u)^2(t^3+9t^2u+17tu^2+7u^3)]\\
&-2Q^6t[s^9(3t-u)+s^8(t^2+3tu+2u^2)-s^7(35t^3+47t^2u-3tu^2-23u^3)-s^6(101t^4
\end{aligned}$$

$+233t^3u+167t^2u^2-9tu^3-44u^4)-s^5(134t^5+422t^4u+528t^3u^2+294t^2u^3+17tu^4$
$-33u^5)-s^4(96t^6+392t^5u+648t^4u^2+620t^3u^3+313t^2u^4+35tu^5-10u^6)-s^3(t+u)^2$
$(30t^5+126t^4u+114t^3u^2+142t^2u^3+15tu^4-u^5)+s^2t(6t^7-22t^6u-130t^5u^2-228t^4u^3$
$-241t^3u^4-161t^2u^5-47tu^6-u^7)+2st^2(t+u)^2(4t^5+2t^4u-17t^3u^2-19t^2u^3-12tu^4$
$-4u^5)+2t^3(t+u)^4(t^3-4tu^2-u^3)]+Q^4[s^{10}(5t^2-8tu-u^2)+2s^9(4t^3-6t^2u-15tu^2$
$-5u^3)-s^8(32t^4+48t^3u+59t^2u^2+54tu^3+35u^4)-4s^7(30t^5+63t^4u+45t^3u^2+10t^2u^3$
$+11tu^4+13u^5)-s^6(179t^6+596t^5u+694t^4u^2+228t^3u^3-120t^2u^4-24tu^5+35u^6)$
$-2s^5(78t^7+404t^6u+756t^5u^2+600t^4u^3+74t^3u^4-132t^2u^5-31tu^6+5u^7)-s^4(t+u)^2$
$(86t^6+516t^5u+768t^4u^2+360t^3u^3-142t^2u^4-32tu^5+u^6)-4s^3t(7t^8+89t^7u+338t^6u^2$
$+596t^5u^3+535t^4u^4+212t^3u^5-t^2u^6-19tu^7-u^8)-s^2t^2(t+u)^2(4t^6+92t^5u+338t^4u^2$
$+444t^3u^3+245t^2u^4+30tu^5-13u^6)-4st^3u(t+u)^4(3t^3+12t^2u+8tu^2+2u^3)-4t^4u^2(t$
$+u)^6]+2Q^2s(s+t+u)^2[s^8u(5t+u)+s^7(2t^3+16t^2u+21tu^2+7u^3)+s^6(5t^4+24t^3u$
$+57t^2u^2+46tu^3+16u^4)+s^5(3t^5+13t^4u+55t^3u^2+79t^2u^3+50tu^4+16u^5)-s^4(t^6+11t^5u$
$+22t^4u^2+4t^3u^3-19t^2u^4-22tu^5-7u^6)-s^3(t^7+15t^6u+70t^5u^2+128t^4u^3+113t^3u^4$
$+37t^2u^5-5tu^6-u^7)-s^2tu(t+u)^2(4t^4+27t^3u+49t^2u^2+26tu^3-u^4)-st^2u^2(t+u)^2$
$(5t^3+19t^2u+18tu^2+6u^3)-2t^3u^3(t+u)^4]-s^2(s+u)(s+t+u)^2[s^7(t^2+4tu+u^2)$
$+s^6(4t^3+19t^2u+18tu^2+5u^3)+2s^5(3t^4+19t^3u+33t^2u^2+21tu^3+5u^4)+2s^4(2t^5$
$+20t^4u+56t^3u^2+58t^2u^3+26tu^4+5u^5)+s^3(t^6+22t^5u+98t^4u^2+156t^3u^3+116t^2u^4$
$+42tu^5+5u^6)+s^2u(t+u)^2(5t^4+30t^3u+33t^2u^2+16tu^3+u^4)+stu^2(t+u)^3(5t^2$
$+7tu+4u^2)+t^2u^3(t+u)^4],$

$A=0.$ (A.8)

$\nu(\overline{\nu})+g\to\nu(\overline{\nu})+c\overline{c}\left[{}^3P_2^{(1)}\right]+g$:

$$F=\frac{4g^4\alpha_s^2a_c^2}{135\pi M^3(Q^2+M_Z^2)^2s^4(s+t)^4(s+u)^4(t+u)^4},$$

$T=-24Q^{10}t^4(s+t)(t+u)[s^3+s^2(3t+4u)+s(3t^2+7tu+5u^2)+t^3+3t^2u+3tu^2+2u^3]$
$+4Q^8t^2[s^8+5s^7(t+u)+2s^6(8t^2+16tu+7u^2)+s^5(28t^3+84t^2u+82tu^2+26u^3)$
$+s^4(61t^4+168t^3u+181t^2u^2+102tu^3+29u^4)+s^3(112t^5+365t^4u+443t^3u^2+241t^2u^3$
$+68tu^4+17u^5)+s^2(t+u)^2(103t^4+234t^3u+146t^2u^2+20tu^3+4u^4)+st(43t^6+229t^5u$
$+498t^4u^2+551t^3u^3+298t^2u^4+66tu^5+7u^6)+t^2(t+u)^2(7t^4+29t^3u+47t^2u^2+47tu^3$
$+4u^4)]-2Q^6t[s^9(4t-2u)+2s^8(8t^2+3tu-5u^2)+s^7(61t^3+94t^2u-7tu^2-28u^3)$
$+s^6(151t^4+443t^3u+319t^2u^2-25tu^3-52u^4)+s^5(225t^5+842t^4u+1102t^3u^2+518t^2u^3$
$-19tu^4-58u^5)+s^4(247t^6+1025t^5u+1648t^4u^2+1210t^3u^3+385t^2u^4+11tu^5-34u^6)$
$+s^3(t+u)^2(180t^5+628t^4u+545t^3u^2+106t^2u^3+38tu^4-8u^5)+s^2t(50t^7+548t^6u$
$+1725t^5u^2+2371t^4u^3+1543t^3u^4+483t^2u^5+92tu^6+8u^7)-2st^2(t+u)^2(6t^5-56t^4u$
$-229t^3u^2-255t^2u^3-68tu^4-16u^5)-2t^3(t+u)^3(3t^4-3t^3u-32t^2u^2-49tu^3-11u^4)]$

$$
\begin{aligned}
&-2Q^4[s^{10}(t^2+10tu+3u^2)+s^9(9t^3+55t^2u+61tu^2+15u^3)+3s^8(4t^4+48t^3u+99t^2u^2\\
&+62tu^3+11u^4)-s^7(64t^5-27t^4u-581t^3u^2-803t^2u^3-355tu^4-42u^5)-s^6(221t^6\\
&+557t^5u-54t^4u^2-1270t^3u^3-1278t^2u^4-437tu^5-33u^6)-s^5(317t^7+1180t^6u\\
&+1263t^5u^2-400t^4u^3-1694t^3u^4-1215t^2u^5-336tu^6-15u^7)-s^4(t+u)^2(266t^6+745t^5u\\
&+340t^4u^2-464t^3u^3-408t^2u^4-141tu^5-3u^6)-s^3t(128t^8+840t^7u+1933t^6u^2+1756t^5u^3\\
&+69t^4u^4-969t^3u^5-694t^2u^6-219tu^7-28u^8)-s^2t^2(t+u)^2(26t^6+240t^5u+540t^4u^2\\
&+321t^3u^3-111t^2u^4-81tu^5-29u^6)-2st^3u(t+u)^3(17t^4+73t^3u+76t^2u^2+10tu^3+2u^4)\\
&-14t^4u^2(t+u)^6]+2Q^2s[s^{10}(3t^2+8tu+3u^2)+6s^9(3t^3+10t^2u+10tu^2+3u^3)+s^8(54t^4\\
&+228t^3u+346t^2u^2+216tu^3+48u^4)+s^7(93t^5+526t^4u+1105t^3u^2+1061t^2u^3+464tu^4\\
&+75u^5)+s^6(99t^6+764t^5u+2132t^4u^2+2872t^3u^3+1980t^2u^4+652tu^5+75u^6)+s^5(72t^7\\
&+734t^6u+2618t^5u^2+4630t^4u^3+4480t^3u^4+2370t^2u^5+612tu^6+48u^7)+s^4(t+u)^2(36t^6\\
&+404t^5u+1297t^4u^2+1774t^3u^3+1143t^2u^4+332tu^5+18u^6)+s^3(9t^9+188t^8u+1142t^7u^2\\
&+3251t^6u^3+5142t^5u^4+4834t^4u^5+2729t^3u^6+874t^2u^7+128tu^8+3u^9)+2s^2tu(t+u)^2(16t^6\\
&+138t^5u+387t^4u^2+495t^3u^3+311t^2u^4+100tu^5+10u^6)+st^2u^2(t+u)^3(37t^4+161t^3u\\
&+234t^2u^2+127tu^3+29u^4)+14t^3u^3(t+u)^6],\\
L=\;&24Q^{10}t^4(s+t)(t+u)[s^3+s^2(3t+4u)+s(3t^2+7tu+5u^2)+t^3+3t^2u+3tu^2+2u^3]\\
&-2Q^8t^2[s^8+14s^7(t+u)+s^6(55t^2+110tu+53u^2)+2s^5(67t^3+162t^2u+141tu^2+46u^3)\\
&+s^4(254t^4+666t^3u+652t^2u^2+322tu^3+83u^4)+2s^3(160t^5+521t^4u+608t^3u^2+319t^2u^3\\
&+91tu^4+19u^5)+s^2(t+u)^2(230t^4+516t^3u+304t^2u^2+46tu^3+7u^4)+2st(43t^6+229t^5u\\
&+498t^4u^2+551t^3u^3+298t^2u^4+66tu^5+7u^6)+2t^2(t+u)^2(7t^4+29t^3u+47t^2u^2+47tu^3\\
&+4u^4)]+2Q^6t[s^9(3t-u)+s^8(51t^2+37tu-14u^2)+s^7(221t^3+389t^2u+107tu^2-53u^3)\\
&+s^6(467t^4+1269t^3u+1049t^2u^2+155tu^3-92u^4)+s^5(610t^5+2090t^4u+2674t^3u^2\\
&+1434t^2u^3+161tu^4-83u^5)+s^4(542t^6+2196t^5u+3484t^4u^2+2782t^3u^3+1115t^2u^4\\
&+125tu^5-38u^6)+s^3(t+u)^2(302t^5+990t^4u+870t^3u^2+342t^2u^3+67tu^4-7u^5)+s^2t(70t^7\\
&+670t^6u+2020t^5u^2+2756t^4u^3+1859t^3u^4+643t^2u^5+127tu^6+7u^7)-2st^2(t+u)^2(6t^5\\
&-56t^4u-229t^3u^2-255t^2u^3-68tu^4-16u^5)-2t^3(t+u)^3(3t^4-3t^3u-32t^2u^2-49tu^3\\
&-11u^4)]-Q^4[s^{10}(13t^2+8tu+7u^2)+2s^9(74t^3+56t^2u+tu^2+19u^3)+s^8(588t^4+880t^3u\\
&+61t^2u^2-118tu^3+89u^4)+4s^7(298t^5+750t^4u+413t^3u^2-161t^2u^3-93tu^4+29u^5)\\
&+s^6(1421t^6+5216t^5u+5998t^4u^2+1312t^3u^3-1504t^2u^4-536tu^5+89u^6)+2s^5(536t^7\\
&+2616t^6u+4606t^5u^2+3264t^4u^3+232t^3u^4-734t^2u^5-209tu^6+19u^7)+s^4(t+u)^2(534t^6\\
&+2328t^5u+2692t^4u^2+896t^3u^3-370t^2u^4-184tu^5+7u^6)+4s^3t(43t^8+397t^7u+1177t^6u^2\\
&+1596t^5u^3+1060t^4u^4+279t^3u^5-55t^2u^6-54tu^7-7u^8)+s^2t^2(t+u)^2(28t^6+444t^5u\\
&+1178t^4u^2+920t^3u^3+103t^2u^4-26tu^5-43u^6)+4st^3u(t+u)^3(17t^4+73t^3u+76t^2u^2\\
&+10tu^3+2u^4)+28t^4u^2(t+u)^6]+2Q^2s[s^{10}(8t^2+11tu+7u^2)+s^9(58t^3+78t^2u+65tu^2\\
&+45u^3)+s^8(177t^4+287t^3u+162t^2u^2+187tu^3+127u^4)+s^7(295t^5+655t^4u+232t^3u^2\\
&-20t^2u^3+313tu^4+205u^5)+s^6(290t^6+925t^5u+438t^4u^2-844t^3u^3-540t^2u^4+308tu^5
\end{aligned}
$$

$+205u^6) + s^5(168t^7 + 776t^6u + 692t^5u^2 - 1164t^4u^3 - 2216t^3u^4 - 930t^2u^5 + 165tu^6 + 127u^7)$
$+s^4(t+u)^2(53t^6 + 247t^5u - 61t^4u^2 - 871t^3u^3 - 719t^2u^4 - 55tu^5 + 45u^6) + s^3(t+u)^2(7t^7$
$+53t^6u - 73t^5u^2 - 531t^4u^3 - 697t^3u^4 - 339t^2u^5 - 17tu^6 + 7u^7) - s^2tu^2(t+u)^3(85t^4 + 274t^3u$
$+227t^2u^2 + 99tu^3 + u^4) - 3st^2u^2(t+u)^4(7t^3 + 33t^2u + 22tu^2 + 6u^3) - 14t^3u^3(t+u)^6]$
$-s^2(s+u)(s+t+u)^2[s^7(7t^2 + 12tu + 7u^2) + s^6(28t^3 + 45t^2u + 50tu^2 + 31u^3) + 2s^5(21t^4$
$+33t^3u + 51t^2u^2 + 69tu^3 + 29u^4) + 2s^4(14t^5 + 24t^4u + 34t^3u^2 + 90t^2u^3 + 94tu^4 + 29u^5)$
$+s^3(7t^6 + 18t^5u - 2t^4u^2 + 60t^3u^3 + 180t^2u^4 + 138tu^5 + 31u^6) + s^2u(t+u)^2(3t^4 - 14t^3u$
$+23t^2u^2 + 36tu^3 + 7u^4) + 3stu^2(t+u)^3(t^2 + 3tu + 4u^2) + 7t^2u^3(t+u)^4],$

$$A = 0. \tag{A.9}$$

$\nu(\overline{\nu}) + g \to \nu(\overline{\nu}) + c\overline{c}\left[{}^1S_0^{(8)}\right] + g$:

$$F = \frac{g^4\alpha_s^2}{12\pi M(Q^2 + M_Z^2)^2 s^4 t(s+t)^2(s+u)^2(t+u)^2},$$
$$T = 9v_c^2Q^2(Q^2t + su)[2Q^4t^2u^2 + 2Q^2stu(st + su + t^2 + tu + u^2) + s^6$$
$$+ 2s^5(t+u) + 3s^4(t+u)^2 + 2s^3(t+u)^3 + s^2(t^4 + 2t^3u + 3t^2u^2 + 2tu^3 + u^4)]$$
$$+ 10a_c^2Q^2s^2t^2(Q^2t + su)(s+t+u)^2,$$
$$L = -9v_c^2Q^4t[2Q^4t^2u^2 + 2Q^2stu(st + su + t^2 + tu + 2u^2) + s^4(t+u)^2$$
$$+ 2s^3(t^3 + 2t^2u + 2tu^2 + u^3) + s^2(t^4 + 2t^3u + 3t^2u^2 + 2tu^3 + 2u^4)]$$
$$- 5a_c^2s^2t(Q^2t + su)^2(s+t+u)^2,$$
$$A = 0. \tag{A.10}$$

$\nu(\overline{\nu}) + g \to \nu(\overline{\nu}) + c\overline{c}\left[{}^3S_1^{(8)}\right] + g$:

$$F = \frac{-g^4\alpha_s^2}{36\pi M(Q^2 + M_Z^2)^2 s^4 t(s+t)^2(s+u)^2(t+u)^2},$$
$$T = 10v_c^2Q^2t\{2Q^6t^2(s^2 + t^2) - Q^4t[s^3(3t - 2u) + 3s^2t(t+u) + 2st^2(t-u) + 2t^3(t+u)]$$
$$+ Q^2s[s^3(t-u)^2 - 2s^2tu(t+u) - st^2u(2t-u) - 2t^3u(t+u)] - s^5(t^2 + tu + u^2)$$
$$- s^4(t+u)^3 - s^3tu(t^2 + 3tu + u^2) - s^2t^2u^2(t+u)\} + 9a_c^2Q^2\{2Q^6t^3u^2 - 2Q^4t^2u[s^3$$
$$- s^2(t+u) + s(t^2 + tu - 2u^2) + 2tu(t+u)] - Q^2st[s^5 + 2s^4(t+u) + s^3(t^2 + 2tu$$
$$+ 3u^2) + 2s^2t(t^2 + 3tu + 2u^2) + s(t^4 + 6t^3u + 15t^2u^2 + 12tu^3 - u^4) + 4tu^2(t^2 + 3tu$$
$$+ 2u^2)] - s^7u - 2s^6u(t+u) - s^5(2t^3 + 5t^2u + 6tu^2 + 3u^3) - 2s^4(t^4 + 4t^3u + 7t^2u^2$$
$$+ 5tu^3 + u^4) - s^3u(3t^4 + 12t^3u + 17t^2u^2 + 10tu^3 + u^4) - 2s^2tu^2(t^3 + 3t^2u + 4tu^2$$
$$+ 2u^3)\},$$
$$L = 5v_c^2Q^4t\{2Q^4t^2(s^2 - 2t^2) - 2Q^2t(s^2 - 2t^2)[s(t-u) + t(t+u)] + s^4(t^2 + u^2)$$
$$+ 2s^3t^2(t+u) + s^2t^2(t^2 + 6tu + u^2) + 4st^3u(t+u)\} - 9a_c^2\{2Q^8t^3u^2 + 2Q^6t^2u[s^3$$
$$+ s^2(t+u) - s(t^2 + tu - 2u^2) - 2tu(t+u)] + Q^4st[s^5 + 2s^4(t+u) + s^3u(t+5u)$$
$$- s^2(2t^3 + 7t^2u + tu^2 - 4u^3) - s(t^4 + 6t^3u + 14t^2u^2 + 8tu^3 - 3u^4) - 4tu^2(t^2 + 3tu$$

$$+2u^2)] - Q^2s^2[s^5(t-u) + s^4(3t^2+tu-2u^2) + s^3(3t^3+8t^2u+4tu^2-3u^3) + s^2(t^4 + 9t^3u+18t^2u^2+8tu^3-2u^4) + su(3t^4+13t^3u+20t^2u^2+9tu^3-u^4) + tu^2(t + u)^2(t+5u)] - s^3u(s+t+u)[s^2+s(t+u)+u(t+u)]^2\},$$

$$A = 0. \tag{A.11}$$

$\nu(\overline{\nu}) + g \to \nu(\overline{\nu}) + c\overline{c}\left[{}^3P_J^{(8)}\right] + g$:

$$F = \frac{-g^4\alpha_s^2}{3\pi M^3(Q^2+M_Z^2)^2s^4t(s+t)^3(s+u)^4(t+u)^3},$$

$$\begin{aligned}T = {} & 9v_c^2Q^2\{8Q^8t^2[2s^5t - 2s^4u^2 + s^3t^2(2t-3u) - s^2tu(t^2+3tu-3u^2) - stu(2t^3+t^2u \\ & - tu^2-u^3) + t^2u^3(2t+u)] - 2Q^6t[4s^7(t+u) + 4s^6(5t^2+2u^2) + 4s^5(5t^3+6t^2u \\ & - 2tu^2+4u^3) + 2s^4(9t^4-9t^3u+4t^2u^2-6tu^3+4u^4) + s^3(12t^5-2t^4u-29t^3u^2 \\ & + 33t^2u^3-12tu^4+4u^5) - s^2t(2t^5+20t^4u+25t^3u^2-t^2u^3-16tu^4+4u^5) - st^2u \\ & \times (12t^4+26t^3u+2t^2u^2+tu^3+u^4) - t^3u^2(2t^3-6t^2u-15tu^2-7u^3)] + 2Q^4[2s^8 \\ & \times (3t^2+tu-2u^2) + s^7(21t^3+3t^2u+10tu^2-8u^3) + s^6(28t^4+15t^3u-15t^2u^2+22tu^3 \\ & - 12u^4) + s^5(27t^5+11t^4u+8t^3u^2-20t^2u^3+26tu^4-8u^5) + s^4(16t^6+17t^5u-20t^4u^2 \\ & + 2t^3u^3-33t^2u^4+18tu^5-4u^6) + s^3t(2t^6+8t^5u-3t^4u^2-19t^3u^3-19t^2u^4-17tu^5 \\ & + 6u^6) - s^2t^2(2t^6+14t^5u+30t^4u^2+33t^3u^3+46t^2u^4+21tu^5+4u^6) - 2st^3u(2t^5 \\ & + 10t^4u+16t^3u^2+20t^2u^3+19tu^4+7u^5) - 2t^6u^2(t+u)^2] - Q^2s[s^8(7t^2-5tu-12u^2) \\ & + s^7(25t^3+3t^2u-18tu^2-36u^3) + s^6(37t^4+25t^3u-12t^2u^2-20tu^3-60u^4) + s^5(39t^5 \\ & + 39t^4u+16t^3u^2-18t^2u^3-6tu^4-60u^5) + s^4(29t^6+83t^5u+72t^4u^2+88t^3u^3+40t^2u^4 \\ & + 22tu^5-36u^6) + s^3(9t^7+75t^6u+148t^5u^2+176t^4u^3+178t^3u^4+102t^2u^5+22tu^6 \\ & - 12u^7) + s^2tu(22t^6+107t^5u+199t^4u^2+211t^3u^3+177t^2u^4+73tu^5+9u^6) + st^2u^2(17t^5 \\ & + 69t^4u+107t^3u^2+105t^2u^3+71tu^4+21u^5) + 4t^5u^3(t+u)^2] - s^2(s+u)[7s^7u(t+u) \\ & + s^6u(25t^2+38tu+21u^2) + s^5(2t^4+47t^3u+88t^2u^2+78tu^3+35u^4) + s^4(4t^5+63t^4u \\ & + 132t^3u^2+156t^2u^3+98tu^4+35u^5) + s^3(2t^6+47t^5u+136t^4u^2+190t^3u^3+156t^2u^4 \\ & + 78tu^5+21u^6) + s^2u(13t^6+70t^5u+136t^4u^2+132t^3u^3+88t^2u^4+38tu^5+7u^6) + stu^2 \\ & \times (13t^5+47t^4u+63t^3u^2+47t^2u^3+25tu^4+7u^5) + 2t^4u^3(t+u)^2]\} + 10a_c^2Q^2t\{4Q^8t^4 \\ & \times [2s^3+s^2(5t+7u)+s(4t^2+11tu+7u^2)+(t+u)^2(t+2u)] + 2Q^6t^2[2s^6+s^5(7t \\ & + 9u) + s^4(5t^2+27tu+12u^2) - s^3(13t^3-7t^2u-34tu^2-4u^3) - s^2(23t^4+57t^3u \\ & + 18t^2u^2-14tu^3+2u^4) - s(12t^5+52t^4u+73t^3u^2+33t^2u^3+tu^4+u^5) - t(2t^5 \\ & + 12t^4u+27t^3u^2+29t^2u^3+13tu^4+u^5)] - Q^4t[2s^7(5t-2u) + s^6(41t^2+37tu-18u^2) \\ & + s^5(56t^3+147t^2u+45tu^2-24u^3) + s^4(19t^4+164t^3u+194t^2u^2+19tu^3-8u^4) \\ & - s^3(16t^5-12t^4u-154t^3u^2-117t^2u^3+5tu^4-4u^5) - s^2(8t^6+66t^5u+95t^4u^2 \\ & + 8t^3u^3-17t^2u^4+10tu^5-2u^6) + 2st(2t^6-8t^5u-53t^4u^2-82t^3u^3-45t^2u^4 \\ & - 8tu^5-2u^6) + 2t^2(t+u)^2(t^4-8t^2u^2-12tu^3-3u^4)] + Q^2[s^9(t+u) + s^8(11t^2 \\ & + tu+6u^2) + s^7(40t^3+36t^2u-3tu^2+17u^3) + s^6(56t^4+144t^3u+57t^2u^2+9tu^3\end{aligned}$$

$$
\begin{aligned}
&+ 24u^4) + s^5(19t^5 + 167t^4u + 230t^3u^2 + 90t^2u^3 + 41tu^4 + 17u^5) - s^4(29t^6 + 5t^5u \\
&- 182t^4u^2 - 228t^3u^3 - 117t^2u^4 - 53tu^5 - 6u^6) - s^3(30t^7 + 126t^6u + 115t^5u^2 \\
&- 81t^4u^3 - 158t^3u^4 - 88t^2u^5 - 31tu^6 - u^7) - s^2t(8t^7 + 72t^6u + 191t^5u^2 + 181t^4u^3 \\
&+ 16t^3u^4 - 60t^2u^5 - 29tu^6 - 7u^7) - 2st^2u(t+u)^2(5t^4 + 21t^3u + 21t^2u^2 + 2tu^3 \\
&- u^4) - 4t^3u^2(t+u)^5] - s(s+u)[s^8(t+u) + 6s^7(t^2 + tu + u^2) + s^6(19t^3 + 29t^2u \\
&+ 27tu^2 + 17u^3) + 2s^5(17t^4 + 47t^3u + 50t^2u^2 + 35tu^3 + 12u^4) + s^4(35t^5 + 162t^4u \\
&+ 254t^3u^2 + 202t^2u^3 + 92tu^4 + 17u^5) + s^3(20t^6 + 145t^5u + 338t^4u^2 + 370t^3u^3 \\
&+ 216t^2u^4 + 65tu^5 + 6u^6) + s^2(5t^7 + 62t^6u + 217t^5u^2 + 346t^4u^3 + 286t^3u^4 + 125t^2u^5 \\
&+ 26tu^6 + u^7) + stu(t+u)^2(9t^4 + 40t^3u + 56t^2u^2 + 28tu^3 + 5u^4) + 4t^2u^2(t+u)^5]\},
\end{aligned}
$$

$$
\begin{aligned}
L = 18v_c^2Q^4\{&4Q^6t^2[s^5t - s^4u^2 - 2s^3t^3 + s^2t^2u(t+3u) + stu(2t^3 + t^2u - tu^2 - u^3) \\
&- t^2u^3(2t+u)] - Q^4t[2s^7(t+u) + 4s^6(2t^2 + u^2) - s^5(t^3 - t^2u + 2tu^2 - 8u^3) - s^4(21t^4 \\
&+ 13t^3u + 18t^2u^2 - 2tu^3 - 4u^4) - 2s^3(6t^5 + 10t^4u + t^3u^2 + 4t^2u^3 - 6tu^4 - u^5) + 2s^2t \\
&\times (t^5 + 10t^4u + 11t^3u^2 + 9t^2u^3 + 6tu^4 + 5u^5) + st^2u(12t^4 + 26t^3u + 2t^2u^2 + tu^3 + u^4) \\
&+ t^3u^2(2t^3 - 6t^2u - 15tu^2 - 7u^3)] + 2Q^2[s^8(t^2 - u^2) + s^7(3t^3 + tu^2 - 2u^3) - s^6(2t^4 \\
&+ 2t^3u + 2t^2u^2 - tu^3 + 3u^4) - s^5(12t^5 + 16t^4u + 16t^3u^2 - t^2u^3 + tu^4 + 2u^5) - s^4(10t^6 \\
&+ 28t^5u + 28t^4u^2 + 13t^3u^3 - 7t^2u^4 + 3tu^5 + u^6) - s^3t(t^6 + 9t^5u + 18t^4u^2 + t^3u^3 \\
&- 15t^2u^4 - 10tu^5 + 2u^6) + s^2t^2(t^6 + 7t^5u + 13t^4u^2 + 18t^3u^3 + 35t^2u^4 + 24tu^5 + 6u^6) \\
&+ st^3u(2t^5 + 10t^4u + 16t^3u^2 + 20t^2u^3 + 19tu^4 + 7u^5) + t^6u^2(t+u)^2] + s(s+u)[2s^7u(t \\
&+ u) + 2s^6u(3t^2 + 3tu + 2u^2) + s^5(5t^4 + 15t^3u + 18t^2u^2 + 14tu^3 + 6u^4) + s^4(15t^5 \\
&+ 38t^4u + 53t^3u^2 + 40t^2u^3 + 22tu^4 + 4u^5) + s^3(15t^6 + 52t^5u + 88t^4u^2 + 81t^3u^3 + 47t^2u^4 \\
&+ 19tu^5 + 2u^6) + s^2t(5t^6 + 32t^5u + 78t^4u^2 + 90t^3u^3 + 68t^2u^4 + 34tu^5 + 9u^6) + st^2u(7t^5 \\
&+ 31t^4u + 47t^3u^2 + 39t^2u^3 + 23tu^4 + 7u^5) + 2t^5u^2(t+u)^2]\} - 10a_c^2t\{4Q^{10}t^4[2s^3 \\
&+ s^2(5t+7u) + s(4t^2 + 11tu + 7u^2) + (t+u)^2(t+2u)] - 2Q^8t^2[2s^6 + 2s^5(4t+5u) \\
&+ 2s^4(9t^2 + 11tu + 9u^2) + s^3(29t^3 + 43t^2u + 15tu^2 + 15u^3) + s^2(27t^4 + 73t^3u + 41t^2u^2 \\
&+ tu^3 + 6u^4) + s(12t^5 + 52t^4u + 73t^3u^2 + 33t^2u^3 + tu^4 + u^5) + t(2t^5 + 12t^4u + 27t^3u^2 \\
&+ 29t^2u^3 + 13tu^4 + u^5)] + Q^6t[s^7(11t - 4u) + 5s^6(9t^2 + 8tu - 4u^2) + s^5(81t^3 + 153t^2u \\
&+ 73tu^2 - 36u^3) + s^4(87t^4 + 221t^3u + 226t^2u^2 + 99tu^3 - 30u^4) + s^3(56t^5 + 198t^4u \\
&+ 231t^3u^2 + 183t^2u^3 + 82tu^4 - 12u^5) + s^2(14t^6 + 106t^5u + 201t^4u^2 + 145t^3u^3 + 69t^2u^4 \\
&+ 31tu^5 - 2u^6) - 2st(2t^6 - 8t^5u - 53t^4u^2 - 82t^3u^3 - 45t^2u^4 - 8tu^5 - 2u^6) - 2t^2(t+u)^2 \\
&\times (t^4 - 8t^2u^2 - 12tu^3 - 3u^4)] - Q^4[s^9(t+u) + s^8(14t^2 - tu + 6u^2) + s^7(48t^3 + 35t^2u \\
&- 18tu^2 + 16u^3) + s^6(78t^4 + 148t^3u + 17t^2u^2 - 54tu^3 + 22u^4) + s^5(75t^5 + 240t^4u + 214t^3u^2 \\
&- 30t^2u^3 - 86tu^4 + 16u^5) + s^4(48t^6 + 229t^5u + 360t^4u^2 + 216t^3u^3 - 43t^2u^4 - 74tu^5 \\
&+ 6u^6) + s^3(20t^7 + 152t^6u + 339t^5u^2 + 326t^4u^3 + 134t^3u^4 - 17t^2u^5 - 31tu^6 + u^7) + s^2t(4t^7 \\
&+ 62t^6u + 210t^5u^2 + 275t^4u^3 + 150t^3u^4 + 28t^2u^5 - 4tu^6 - 5u^7) + 2st^2u(t+u)^2(5t^4 + 21t^3u \\
&+ 21t^2u^2 + 2tu^3 - u^4) + 4t^3u^2(t+u)^5] + Q^2s[2s^9(t+u) + s^8(12t^2 + 12tu + 13u^2) + s^7(28t^3 \\
&+ 41t^2u + 37tu^2 + 37u^3) + s^6(32t^4 + 73t^3u + 50t^2u^2 + 62tu^3 + 60u^4) + s^5(18t^5 + 59t^4u
\end{aligned}
$$

$$+ 29t^3u^2 - 17t^2u^3 + 48tu^4 + 60u^5) + s^4(4t^6 + 11t^5u - 41t^4u^2 - 146t^3u^3 - 133t^2u^4 + 2tu^5$$
$$+ 37u^6) - s^3u(10t^6 + 84t^5u + 225t^4u^2 + 279t^3u^3 + 162t^2u^4 + 21tu^5 - 13u^6) - s^2u(t+u)^2$$
$$\times (4t^5 + 40t^4u + 87t^3u^2 + 57t^2u^3 + 16tu^4 - 2u^5) - 2stu^2(t+u)^3(4t^3 + 15t^2u + 9tu^2 + u^3)$$
$$- 4t^2u^3(t+u)^5] - s^2(s+u)(s+t+u)^2[s^6(t+u) + s^5(3t^2 + 4tu + 4u^2) + s^4(3t^3 + 7t^2u$$
$$+ 11tu^2 + 7u^3) + s^3(t^4 + 6t^3u + 13t^2u^2 + 14tu^3 + 7u^4) + s^2u(2t^4 + 8t^3u + 13t^2u^2 + 11tu^3$$
$$+ 4u^4) + su^2(t+u)^2(2t^2 + 2tu + u^2) + tu^3(t+u)^3]\},$$
$$A = 0. \tag{A.12}$$

References

[1] G.T. Bodwin, E. Braaten, G.P. Lepage, Phys. Rev. D 51 (1995) 1125;
G.T. Bodwin, E. Braaten, G.P. Lepage, Phys. Rev. D 55 (1997) 5853, Erratum.

[2] E.L. Berger, D. Jones, Phys. Rev. D 23 (1981) 1521;
R. Baier, R. Rückl, Phys. Lett. 102 B (1981) 364;
R. Baier, R. Rückl, Z. Phys. C 19 (1983) 251;
B. Humpert, Phys. Lett. B 184 (1987) 105;
R. Gastmans, W. Troost, T.T. Wu, Phys. Lett. B 184 (1987) 257;
R. Gastmans, W. Troost, T.T. Wu, Nucl. Phys. B 291 (1987) 731.

[3] E. Braaten, S. Fleming, Phys. Rev. Lett. 74 (1995) 3327;
E. Braaten, T.C. Yuan, Phys. Rev. D 52 (1995) 6627;
P. Cho, A.K. Leibovich, Phys. Rev. D 53 (1996) 150;
P. Cho, A.K. Leibovich, Phys. Rev. D 53 (1996) 6203.

[4] CDF Collaboration, F. Abe et al., Phys. Rev. Lett. 69 (1992) 3704;
CDF Collaboration, F. Abe et al., Phys. Rev. Lett. 71 (1993) 2537;
CDF Collaboration, F. Abe et al., Phys. Rev. Lett. 79 (1997) 572;
CDF Collaboration, F. Abe et al., Phys. Rev. Lett. 79 (1997) 578;
D0 Collaboration, S. Abachi et al., Phys. Lett. B 370 (1996) 239;
D0 Collaboration, B. Abbott et al., Phys. Rev. Lett. 82 (1999) 35.

[5] E. Braaten, S. Fleming, T.C. Yuan, Ann. Rev. Nucl. Part. Sci. 46 (1996) 197;
B.A. Kniehl, G. Kramer, Phys. Lett. B 413 (1997) 416;
M. Krämer, Prog. Part. Nucl. Phys. 47 (2001) 141.

[6] M. Beneke, M. Krämer, Phys. Rev. D 55 (1997) 5269;
A.K. Leibovich, Phys. Rev. D 56 (1997) 4412;
M. Beneke, M. Krämer, M. Vänttinen, Phys. Rev. D 57 (1998) 4258;
B.A. Kniehl, J. Lee, Phys. Rev. D 62 (2000) 114027;
S. Fleming, A.K. Leibovich, I.Z. Rothstein, Phys. Rev. D 64 (2001) 036002.

[7] E. Braaten, B.A. Kniehl, J. Lee, Phys. Rev. D 62 (2000) 094005.

[8] Š. Todorova-Nová, in *Proceedings of the XXXI International Symposium on Multiparticle Dynamics*, September 1–7, 2001, Datong, China (World Scientific, Singapore, to appear), Report No. hep-ph/0112050.

[9] M. Klasen, B.A. Kniehl, L.N. Mihaila, M. Steinhauser, Report No. DESY 01-202, hep-ph/0112259.

[10] CDHS Collaboration, H. Abramowicz et al., Phys. Lett. 109 B (1982) 115.

[11] NuTeV Collaboration, T. Adams et al., Phys. Rev. D 61 (2000) 092001.

[12] CHORUS Collaboration, E. Eskut et al., Phys. Lett. B 503 (2001) 1.

[13] M. Mezzetto, on behalf of the NOMAD Collaboration, Nucl. Phys. B (Proc. Suppl.) 91 (2001) 184;
K. Zuber, private communication.

[14] M.K. Gaillard, S.A. Jackson, D.V. Nanopoulos, Nucl. Phys. B 102 (1976) 326;
M.K. Gaillard, S.A. Jackson, D.V. Nanopoulos, Nucl. Phys. B 112 (1976) 545, Erratum.

[15] J.H. Kühn, R. Rückl, Phys. Lett. 95 B (1980) 431.

[16] J.H. Kühn, Acta Phys. Polon. B 12 (1981) 347.

[17] V. Barger, W.Y. Keung, R.J.N. Phillips, Phys. Lett. 92 B (1980) 179.

[18] H. Fritzsch, Phys. Lett. 67 B (1977) 217;
F. Halzen, Phys. Lett. 69 B (1977) 105.

[19] R. Baier, R. Rückl, Nucl. Phys. B 201 (1982) 1.

[20] L.M. Sehgal, Prog. Part. Nucl. Phys. 14 (1985) 1.

[21] Particle Data Group, D.E. Groom et al., Eur. Phys. J. C 15 (2000) 1.

[22] B.A. Kniehl, L. Zwirner, Nucl. Phys. B 621 (2002) 337.

[23] A.A. Petrov, T. Torma, Phys. Rev. D 60 (1999) 093009.

[24] E. Braaten, Y.-Q. Chen, Phys. Rev. D 55 (1997) 2693.

[25] A. Petrelli, M. Cacciari, M. Greco, F. Maltoni, M.L. Mangano, Nucl. Phys. B 514 (1998) 245;
F. Maltoni, M.L. Mangano, A. Petrelli, Nucl. Phys. B 519 (1998) 361.

[26] L.N. Hand, Phys. Rev. 129 (1963) 1834.

[27] New Muon Collaboration, M. Arneodo et al., Phys. Lett. B 332 (1994) 195.

[28] Fermilab E203 Collaboration, A.R. Clark et al., Phys. Rev. Lett. 43 (1979) 187.

[29] T. Weiler, Phys. Rev. Lett. 44 (1980) 304.

[30] M. de Jong, PhD Thesis, Free University of Amsterdam, 1991.

[31] R.L. Anderson et al., Phys. Rev. Lett. 38 (1977) 263.

[32] Tagged-Photon Spectrometer Collaboration, M.D. Sokoloff et al., Phys. Rev. Lett. 57 (1986) 3003.

[33] European Muon Collaboration, J.J. Aubert et al., Phys. Lett. 152 B (1985) 433.

[34] New Muon Collaboration, P. Amaudruz et al., Nucl. Phys. B 371 (1992) 553.

[35] Fermilab E706 Collaboration, L. Apanasevich et al., Phys. Rev. Lett. 81 (1998) 2642.

[36] A.D. Martin, R.G. Roberts, W.J. Stirling, R.S. Thorne, Eur. Phys. J. C 4 (1998) 463.

[37] CTEQ Collaboration, H.L. Lai et al., Eur. Phys. J. C 12 (2000) 375.

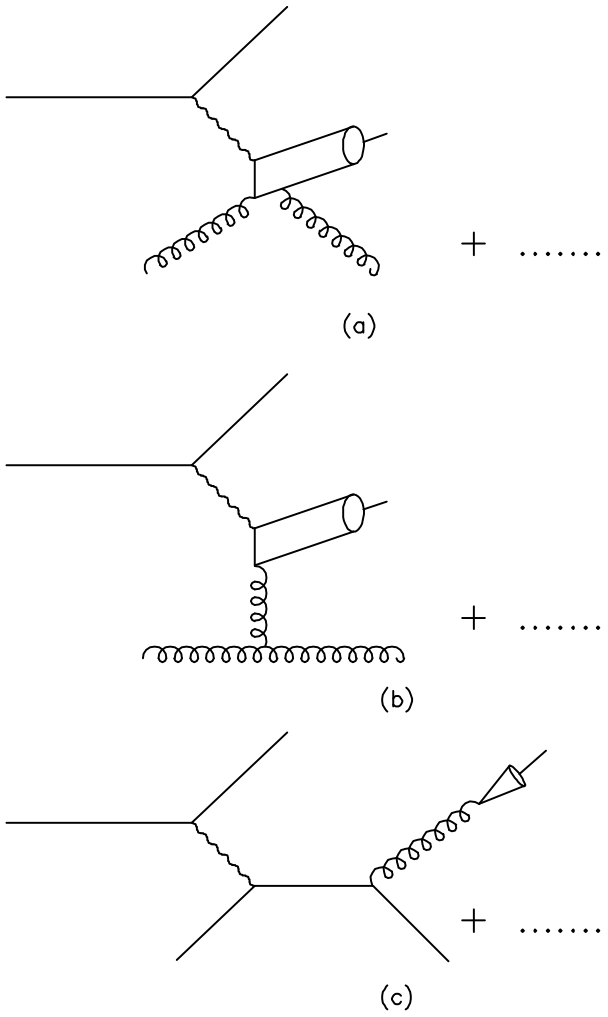

Figure 1: Representative Feynman diagrams for the partonic subprocesses $\nu + a \to \nu + c\overline{c}[n] + a$, where $a = q, \overline{q}, g$ and $n = {}^3S_1^{(1)}, {}^3P_J^{(1)}, {}^1S_0^{(8)}, {}^3S_1^{(8)}, {}^3P_J^{(8)}$. There are six diagrams of the type shown in part (a), two ones of the type shown in part (b), and two ones of the type shown in part (c). There are two more diagrams that are obtained from the diagrams of the type shown in part (b) by replacing the external gluon lines with quark ones. The CS process only proceeds through the diagrams shown in part (a).

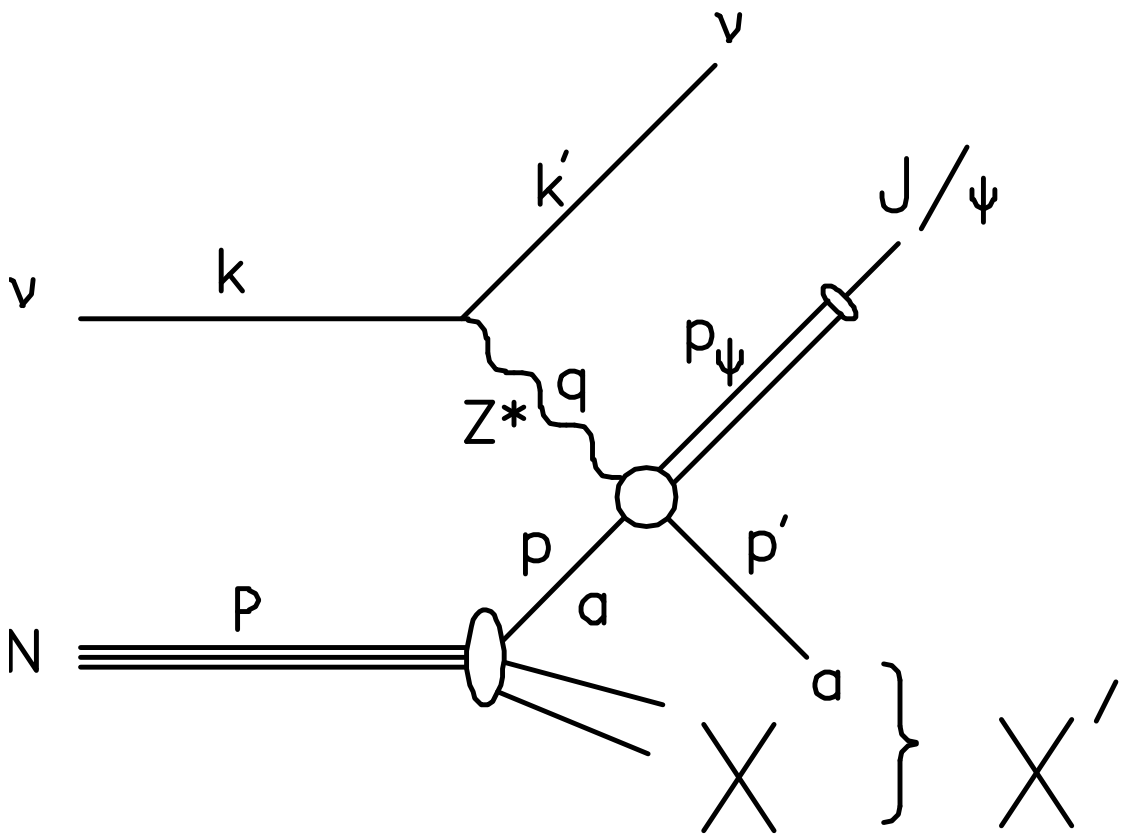

Figure 2: Schematic representation of $\nu + N \rightarrow \nu + J/\psi + j + X$ explaining the four-momentum assignments.

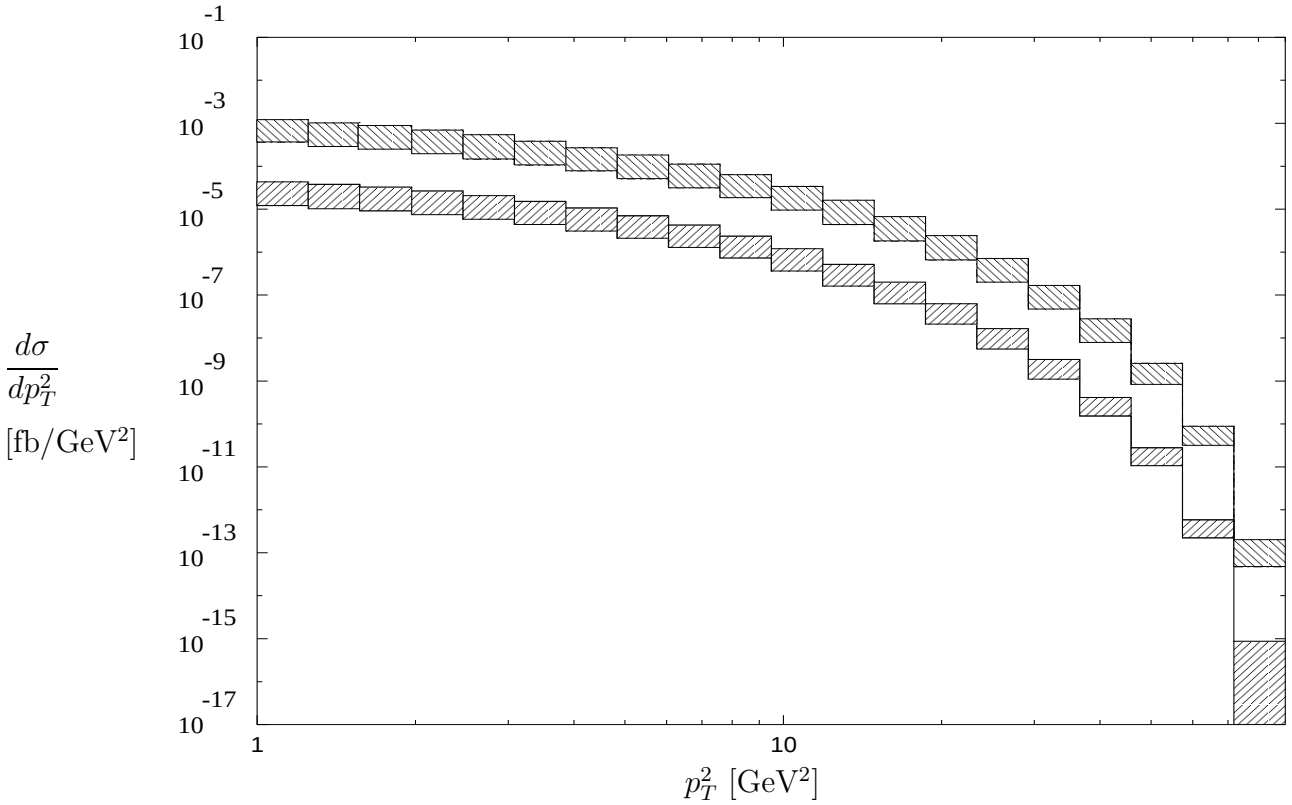

Figure 3: LO NRQCD (upper histogram) and CSM (lower histogram) predictions for the p_T^2 distribution of prompt J/ψ inclusive production in nondiffractive νN NC DIS appropriate for the CHORUS and NOMAD experiments.

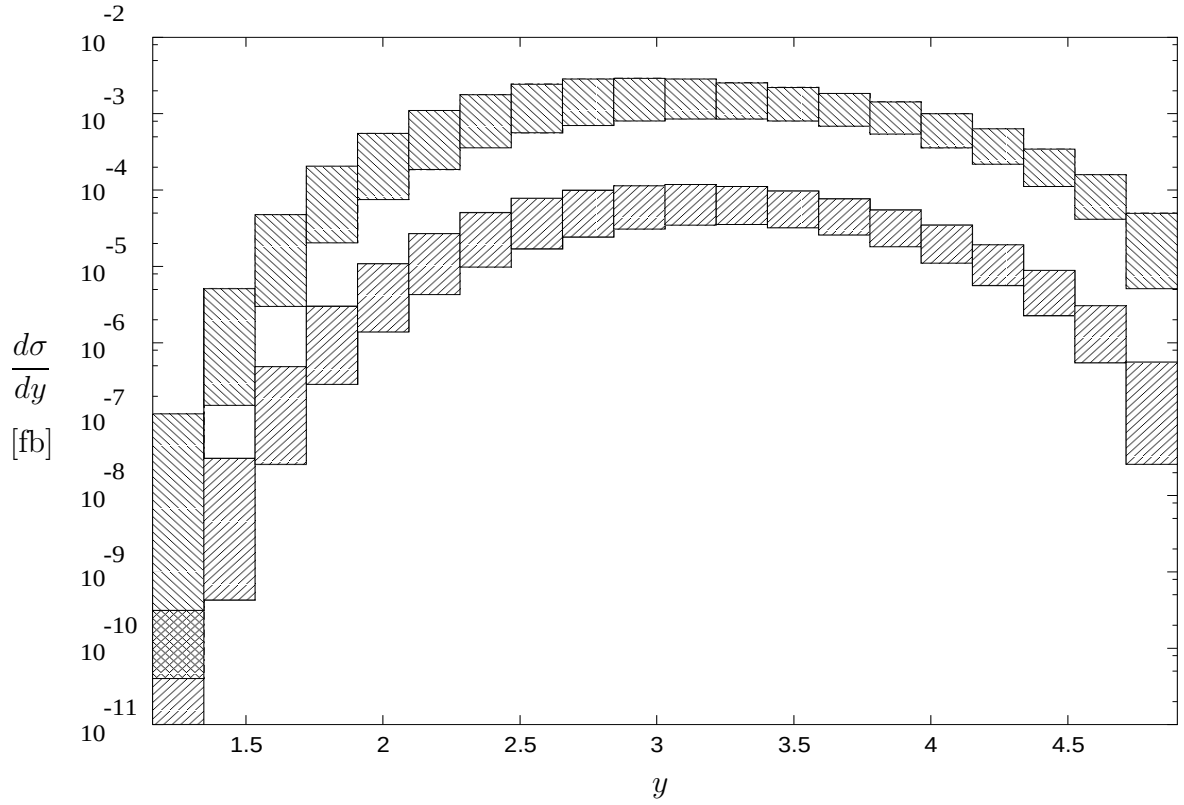

Figure 4: LO NRQCD (upper histogram) and CSM (lower histogram) predictions for the y distribution of prompt J/ψ inclusive production in nondiffractive νN NC DIS appropriate for the CHORUS and NOMAD experiments.

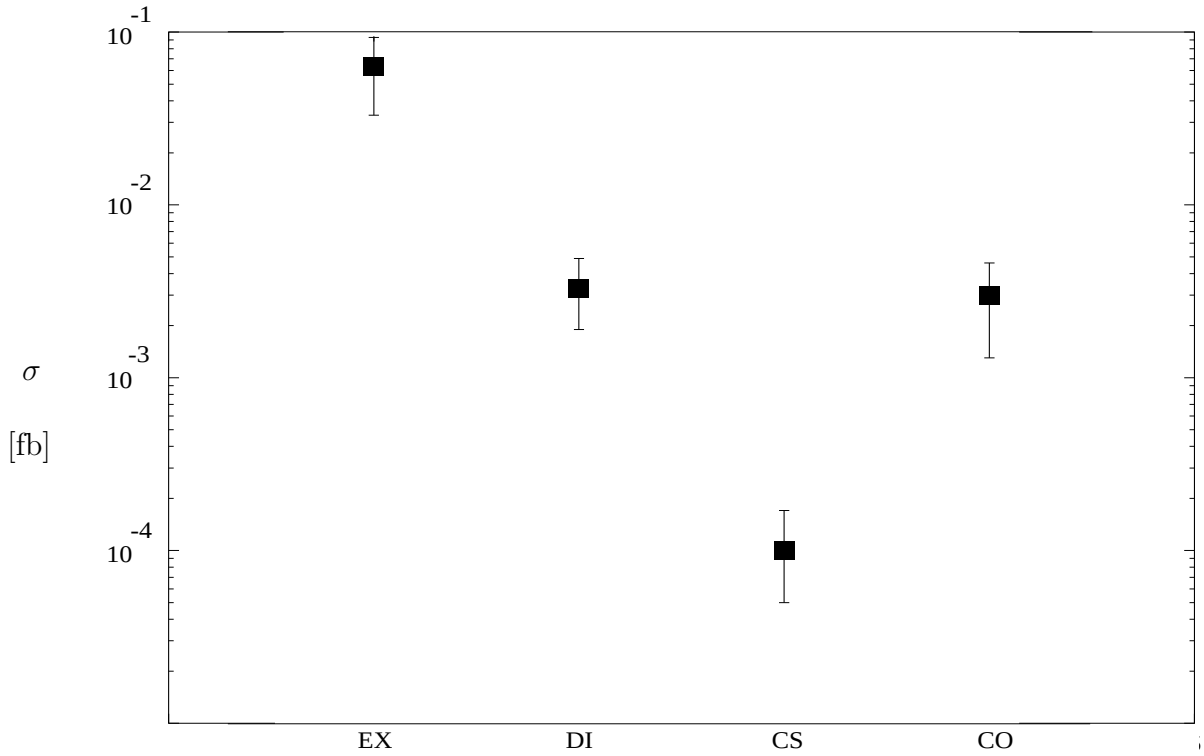

Figure 5: The total cross section of $\nu + N \to \nu + J/\psi + X$ measured by CHORUS [12] (EX) is compared with the predicted diffractive (DI), CS, and CO contributions.